SYNAPTIC PLASTICITY IN MURINE AUTISM SPECTRUM DISORDER MODELS:

AN ELECTROPHYSIOLOGICAL PERSPECTIVE

Amanda Jass

A THESIS SUBMITTED TO THE FACULTY OF
GRADUATE STUDIES IN PARTIAL FULFILLMENT
OF THE REQUIREMENTS FOR THE DEGREE OF
MASTER OF SCIENCE

GRADUATE PROGRAM IN BIOLOGY
YORK UNIVERSITY
TORONTO, ONTARIO

June 2021

Abstract

Changes in synaptic strength of small neuronal populations are difficult to observe in the live human brain; however, these alterations are necessary to study in order to better understand the mechanisms that underlie neurodevelopmental disorders, such as autism spectrum disorder (ASD). Substituting the mouse brain for experimental study in this area is beneficial because mice have similar brain structures and genes homologous to humans. Through manipulation of genes and environmental toxin exposure implicated in the etiology of ASD, we can generate ASD mouse models suitable for gaining insight into synaptic plasticity abnormalities and strategies for restoration. In the following report, I explore how to set up electrophysiology equipment for efficient measure of neuronal population responses in the mouse hippocampus. I then characterize synaptic plasticity aberrations in the prostaglandin E_2 (PGE_2) mouse model of ASD, a developmental toxins model whereby the pregnant mouse is injected with PGE_2. The offspring of PGE_2-injected mice were found to have diminished baseline synaptic response and enhanced potentiation during the first 10 minutes following single-train, high-frequency stimulus in the CA3-CA1 region of the hippocampus. Lastly, I discuss therapeutic applications and the need to further investigate synaptic plasticity in a variety of ASD mouse models.

Acknowledgments

For your guidance and support throughout this journey, thank you to my supervisor Dr. Steven Connor, my advisor Dr. Jennifer Steeves, the current and previous members of my research lab – Sandra Bak, Michael Udom, Raman Abbaspour, Parisa Tari, Georg S. Zoidl, and Olga Fedorets – and my PGE_2 project collaborators Dr. Dorota Anna Crawford, Ashby Kissoondoyal, and Shalini Iyer.

For helping me stay "on track" and motivated during the zombie apocalypse, thank you to my COVID-19 Partners on Track team – Elia Grieco, Chun Chih Chen, Pavan Singh, Jay Kwon, Henry Cameron, and Aarun Verma.

Statement of Contribution

Electrophysiology experiments were conducted by Amanda Jass. PGE_2-injected mouse models were generated by Ashby Kissoondoyal.

Table of Contents

List of Tables

List of Figures

CHAPTER 1: BACKGROUND INFORMATION

GENERAL INTRODUCTION

The mammalian brain is comprised of an elaborate network of neural connections capable of change and regeneration over time. This ability to augment form and function of neurons, networks, and whole brain structures is known collectively as brain plasticity. The core mechanisms that allow for brain plasticity exist at the synaptic level, the point of signal transfer between two neurons. Activity at the neuronal junction or "synapse" is thought to regulate synaptic plasticity, which is defined as the strengthening or weakening of neural connections at the cellular level. Aberrant synaptic plasticity has been implicated in a number of psychiatric disorders including Alzheimer's disease, Parkinson's disease, schizophrenia, and autism spectrum disorder (ASD) (Taoufik *et al*., 2018).

ASD is currently the fastest-growing neurodevelopmental disorder in North America (Christensen *et al*., 2018; Ofner *et al*., 2018). Approximately 1 in 66 Canadians aged 5-17 are diagnosed with ASD (Ofner *et al*., 2018), a disorder characterized by impairments in communication, lack of social interaction, and repetitive, stereotyped behaviour (Ousley & Tracy, 2014). The role of synaptic plasticity in autism is of particular significance because this disorder is marked by imbalances of excitatory to inhibitory synapses (E/I ratio) (Nelson & Valakh, 2015). For instance, there is evidence of over-excitation in the brains of those with ASD (Takarae & Sweeney, 2017), and reports indicate frequent co-occurrence with seizures (an outcome of hyper-excitation) (Tuchman & Rapin, 2002). Additionally, common mutations in genes that code for synapse organizing proteins have been discovered in a disproportionate amount of autism cases (Bucan *et al.,* 2009*)*. Thus, there is growing interest in identifying how

exactly synaptic plasticity is altered in ASD, with the intent of developing ways to restore synaptic balance and thereby mitigate symptomology.

1.1 Synaptic plasticity and autism spectrum disorder

Although the origin of plasticity in relation to the nervous system remains unclear, one of the earliest records of this concept was put forth by Santiago Ramon y Cajal, a Spanish neuroscientist who is considered by many to be the father of modern neuroscience. In 1892, he presented a theory called the *cerebral gymnastics hypothesis*, which proposed that the strength between neurons could increase with exposure to certain stimuli by development of additional connections (Cajal, 1892). However, despite this theory, Cajal's stance on brain plasticity is difficult to interpret, because in some instances he seemed to agree with the prevailing dogma that neurons in the adult brain are fixed and unchanging. For example, he also claimed that 'once development was ended [neuronal] growth…dried up irrevocably' (Cajal, 1913). The actual term "plasticity" in reference to the nervous system is thought to come from Ernesto Lugaro, an Italian psychiatrist (Berlucchi, 2002). In 1906, he proposed that chemotropic activities lead to organized changes of the nervous system throughout the life span. He was inspired by his teacher Eugenio Tanzi, who predicted in 1893 that memories are formed by decreasing the distance between neurons through growth in neuronal length (Berlucchi, 2002). Although the idea of synaptic plasticity was suggested prior to and during the early 20th century, it was not widely accepted, and many people assumed that the adult brain could not change in any capacity beyond degeneration with age (Gage, 2004). A paradigm shift in thinking then took place in 1949, when Donald Hebb, a Canadian psychologist, outlined his theory on synaptic plasticity in his book *The Organization of Behaviour*. In an attempt to explain how learning takes place at all ages, he stated that, "When an axon of cell *A* is near enough to excite a cell *B* and repeatedly or

persistently takes part in firing it, some growth process or metabolic change takes place in one or both cells such that *A*'s efficiency, as one of the cells firing *B*, is increased" (Hebb, 1949; page 62). This pivotal hypothesis suggested that synaptic efficiency arises from repeated activity among pre- and postsynaptic neurons, and it helped spark interest in adult neuroplasticity. Two decades later, in 1973, Hebb's postulate was confirmed with experimental evidence in a landmark study by neuroscientists Tim Bliss and Terje Lømo. They demonstrated that when neurons are stimulated with brief high-frequency electrical pulses, which mimic the neuronal action potential, a long-lasting state of heightened excitability can be induced (Bliss & Lømo, 1973). Using live rabbits anesthetized with urethane, they incorporated a two-microelectrode set-up to stimulate the axons of the perforant path (a neuronal pathway in the hippocampus of the brain) and to record subsequent postsynaptic activity. They found that changing the rate of stimulation could alter neuronal strength, where increased firing rate led to heightened synaptic response. Additionally, they showed that repeated trains of stimuli applied over time evoked increased strength of nerve impulses (potentiation). It was from these experiments that the concept of long-term potentiation (LTP), referring to the phenomena of heightened excitability following a recent stimulus, came to light as a model for Hebb's theory. It confirmed that prior activity between neurons does indeed strengthen their synaptic efficacy.

It was later found that LTP differs depending on the amount and intensity of the stimulus applied, and thus can be divided into two distinct phases – early (E-LTP), and late (L-LTP) (Huang, 1998). For instance, E-LTP can be induced by one train of stimuli whereas L-LTP requires multiple repeated trains. Not only are the induction processes distinct, but so are the mechanisms underlying each type of LTP; E-LTP is thought to occur by modification of pre-existing connections, while L-LTP involves gene activation and new synapse formation (Kandel,

2001). E-LTP is similar to short-term memory, whereas L-LTP appears more similar to long-term memory. For example, synaptic strength after 1 train of stimuli decays within a few hours, while multiple trains induce synaptic strength that is stable over many hours (Huang, 1998).

The reverse process of LTP is known as long-term depression (LTD), which is defined as an activity-dependent decrease in synaptic strength (Bliss, 2011). Unlike LTP, the exact origin of the concept of LTD is obscure; however, one of the earliest studies demonstrating LTD arose in 1980 by German Barrionuevo and his research team. They conducted electrophysiological studies using live male rats anesthetized with Nembutal (Barrionuevo *et al.*, 1980). A low-frequency electrical stimulus was applied to the CA1-CA3 hippocampal region with and without prior high-frequency LTP treatment. They observed a significant reduction of potentiated response in the group that received the previous LTP induction. In contract, there was no significant difference when a low-frequency stimulus was applied to the group that did not receive LTP induction. This clearly indicated that LTP can be reversed, and it provided one of the first observable demonstrations of LTD as a process in specific opposition to LTP. It has since been theorized that LTD serves as a model for the process of forgetting (Tsumoto, 1993), while LTP forms the basis of learning and memory (Lynch, 2004). Impairments in both LTP and LTD have been implicated in autism.

Autism spectrum disorder as a medical diagnosis is a relatively recent development; however, it is likely that autism cases existed without label throughout human history. One of the first documented cases of autism comes from J.M.G. Itard's 19th century account of Victor of Aveyron (Wing, 1997). Victor was found as a child of about 12 years old living on his own in the wilderness of France. He was adopted by Itard, a French physician, who provided him with education and documented his behaviour with detailed written descriptions. Itard described

Victor as having a shifting and expressionless gaze, rocking back and forth, lacking social attachment as well as ability to speak, and having a great sense of order (Wolff, 2004), which are all traits that conform to a present-day autism diagnosis. The actual term "autism" was first described in 1908 by psychiatrist Eugen Bleuler as a subcategory of schizophrenia in which individuals were excessively withdrawn and out of touch with the external world. The term was based on the Greek word "autos" meaning self, reflecting the characteristic egocentric nature of ASD (Greydanus, & Toledo-Pereyra, 2012). In 1943, Leo Kanner, an American-Austrian psychiatrist, conducted case studies on 11 children with similar autistic features (Kanner, 1943). He described all cases as falling under a unique category of disorder, which he referred to as 'inborn autistic disturbances of affective contact.' Common symptoms among these children included stereotypy (repetitive acts), echolalia (repetition of words), lack of social attachment, and preference for objects over people. Interestingly, he noted that many of the families from which these children came from were cold and dysfunctional, indicating that lack of warmth in parenting style may be a contributing factor; however, it has since been accepted that parenting style does not cause autism (Ventola *et al*., 2017). In 1944, Hans Asperger, an Austrian pediatrician, independently reported on a group of children with similar characteristics as described by Kanner a year prior; although, the group that Asperger described had less severe symptoms, including one-sided conversations, lack of empathy, and difficulty forming friendships (Asperger, 1944). Autism first appeared in the 3rd version of the Diagnostic and Statistical Manual of Mental Disorders (DSM-3) in 1980, officially making it a stand-alone disorder separate from schizophrenia. Then in 1994, the 4th edition of the DSM (DSM-4) divided autism into subtypes, such as Asperger syndrome (AS) and pervasive developmental disorder-not otherwise specified (PDD-NOS), which helped distinguish individuals on different levels of the

autism spectrum. In 2013, the DSM-5 collapsed all autism subtypes into one diagnosis called 'autism spectrum disorder.' Thus, today both high- and low-functioning individuals on the autism spectrum are grouped together under the single label of ASD. This broadening of the diagnostic label has likely contributed to the increasing rates of ASD diagnosis. However, there is some concern that the rising rates of autism may be connected to environmental contaminants, such as heavy metal poisoning. For example, a 2013 study by Al-Farsi *et al*. found that children with ASD had higher levels of heavy metal exposure. Using mass spectrometry, they analyzed hair samples from 27 ASD children and compared the results to 27 matched non-ASD controls, accounting for age, gender, ethnicity, socio-demographic background, and diet. Heavy metals such as aluminum, chromium, cadmium, cobalt, nickel, boron, and barium were all significantly higher in the ASD group. It is of importance to note: the authors of this study conclude that these findings do not necessarily indicate that heavy metals contribute to pathophysiology, and there continues to be a great deal of ambiguity in relation to the role of the environment in causing ASD. Nonetheless, autism continues to have a profound impact, affecting approximately 7.7 million people worldwide. The aim of synaptic plasticity research in ASD is to uncover the unique neural basis of this disorder, leading to improvement and development of plasticity-based therapeutics.

1.2 Brain morphology and synaptic plasticity in autism

Distinct differences are often observed in the brain morphology and neural circuitry of those with ASD, constituting anomalies that likely have an impact on synaptic efficiency. At the cellular level, there is evidence of aberrant neuronal number and organization. For instance, a study by Courchesne *et al*. (2001) used stereological analysis to count the number of neurons in post-mortem prefrontal tissue of 7 autistic and 6 control males aged 2-16 years old. They found that

the autistic group had significantly more neurons in the prefrontal cortex; however, these results must be interpreted with caution due to limited sample size. The authors speculate that this could be caused by failure of apoptotic mechanisms to remove subplate neurons in early postnatal life. Another study by Hutsler *et al*. (2007) found differences in cortical thickness and patterning. Using Nissl-stain sectioning, they analyzed the post-mortem cortex of 8 ASD individuals and 8 age-matched controls. They found that, in some ASD cases, cortical patterning was similar to controls, but in a select few there were abnormal layer boundaries, neuronal clumping, and increased neuron number. That some ASD cases had normal cortical patterns, while others did not, highlights how ASD can manifest in a variety of ways, and brain structure abnormalities can differ on a case-by-case basis. Additionally, this study noted an age-dependent effect, where cortical thickness decreases significantly with increasing age in autism. In addition to direct neuronal abnormalities, protein markers of neuronal deficits have also been observed in the cerebral spinal fluid (CSF) of ASD individuals. Using an enzyme-linked immunosorbent assay (ELISA), a study by Ahlsén *et al*. (1993) found increased amounts of glial fibrillary acid (GFA) protein in the CSF. Heightened GFA serves as a marker for brain abnormalities, including nerve cell death, brain degeneration, and/or increased turnover of central nervous system synapses.

Modifications at the neural and synaptic level likely contribute to overall structural changes, such as alterations in brain and skull size. For example, a study by Hazlett *et al*. (2005) used magnetic resonance imaging (MRI) and retrospective data to compile head circumference measures from 164 ASD children and 214 non-ASD controls. They found that ASD individuals had significantly larger head circumferences. Additionally, they also observed that the growth trajectory of the head in ASD is relatively normal during the first 12 months of development, but after one year of age it begins growing at an enhanced rate. Furthermore, another study

uncovered several forebrain structure alterations in infantile autism; Gaffney *et al*. (1989) used MRI imaging in 13 autism subjects, and found larger lateral ventricles, larger anterior horns, and a smaller right lenticular nucleus.

Prominent structural changes likely contribute to functional aberrations and symptoms. For instance, one study linked learning deficits in ASD to hippocampal abnormalities; Cooper *et al*. (2017) used functional magnetic resonance imaging (fMRI) to observe brain activity in 24 ASD individuals and 24 controls while the subjects performed a memory encoding and retrieval task. The fMRI results revealed that the ASD group had reduced left prefrontal cortex activity during memory retrieval, and hippocampal reduction in functional connectivity to the inferior/middle frontal gyrus, a pathway thought to allow for monitoring of recollected information. It was also found that the ASD group had reduced success in the retrieval phase of the experiment.

Synaptic pathologies also contribute to the formation of unstable cortical networks. A study by Lewne *et al*. (1999) used non-invasive magnetoencephalography to evaluate patterns of heightened activity (epileptic form activity) in 50 autistic children during stage 3 sleep. They found that 68% had epileptic form activity, indicating that in some cases ASD is marked by hyper-excitability of cortical networks. This implied that there may be an unbalanced ratio of excitatory to inhibitory synapses (E/I ratio). The E/I ratio hypothesis was strongly supported by Antoine *et al*. (2019) in a study demonstrating that multiple types of autism mouse models display reduced inhibitory synaptic response leading to overall increase of E/I ratio. The four genetically altered mouse models tested in this study included $Fmr1^{-/y}$, $Cntnap2^{-/-}$, $16p11.2^{del-/+}$, and $Tsc2^{+/-}$; however, these are just a few of the many genes implicated in autism. Genome-wide analyses of individuals with ASD reveal hundreds of implicated genes, many of which are

involved in synaptic organization (Bucan *et al.,* 2009). To better understand synaptic plasticity in ASD, structural aberrations as well as genetic changes must be considered.

1.3 Autism genes and synapse organization

When Leo Kanner first described the features of autism in 1943, he hinted at a genetic influence when he wrote, "…these children have come into the world with innate inability to form the usual, biologically provided affective contact with people" (Kanner, 1943). To investigate the genetic component of ASD, psychiatrists Susan Folstein and Michael Rutter conducted twin studies in 1977. They examined 21 pairs of twins, where at least one sibling had autism; 11 pairs were monozygotic (sharing 100% of the same genes), and 10 pairs were dizygotic (sharing 50% of the same genes). They found that 4/11 of the monozygotic twins were concordant for autism, while 0/10 of the dizygotic twins were concordant, representing an almost significant finding ($P = 0.055$) in favour of a genetic influence. Then in 2011, another twin study was conducted by Hallmayer *et al*., and this study found a definitive genetic influence in autism. They used a much larger sample size, consisting of 192 twin pairs, where 54 were monozygotic and 138 were dizygotic. Concordance rates for ASD were reported as 77% among the monozygotic pairs and 31% among the dizygotic pairs, representing a significant factor of genetic heritability. Although twin studies could indicate an overall influence of genetics, these studies could not answer precisely which genes were responsible for this effect. To determine the specific genes involved in this disorder, genome-wide scans for autism-susceptibility genes would be required.

The first genome-wide scan for autism genes was conducted by the International Molecular Genetic Study of Autism Consortium in 1998 (Bailey *et al*., 1998). To help ensure that testing covered ASD individuals demonstrating a genetic influence (rather than environmental), only relative-pairs, where both members were affected by ASD, were included. Using a

fluorescence-based semi-automatic genotyping method on 99 familial ASD-pairs, several loci of interest were identified including a notable region on chromosome 7q. However, in this study, only general regions were identified, which contain multiple potential candidate genes. Thus, further fine mapping would be required to refine the analysis to the single gene level. A year later, in 1999, Philippe *et al*. conducted another genome-wide autism scan. Using a similar method, they analyzed the genomes of 51 ASD relative-pairs. They found 11 chromosomal regions positively linked to autism, including the region on chromosome 7q identified in the earlier study. In 2009, Bucan *et al*. conducted a more refined genome-wide analysis for exon copy number variants in ASD. They used a much larger sample size (ASD cases from 912 different families, and 1488 healthy controls), and included an additional independent replication cohort to ensure accuracy. They identified specific autism-susceptibility genes by observation of exon deletions and duplications present in ASD subjects. Interestingly, they identified a number of genes that have a known role in synapse organization, including neurexin-1 (*Nrxn1*), neuroligin-1 (*Nlgn1*), and MAM domain containing glycosylphosphatidylinositol anchor-2 (*Mdga2*). At the synapse, NRXNs and NLGNs function as cell-adhesion proteins, helping to keep pre- and postsynaptic neurons in contact. NLGNs are located on the postsynaptic membrane and physically bind to NRXNs located on the presynaptic membrane. MDGA2 regulates this interaction by selectively binding to NLGN, preventing NLGN-NRXN association (Connor *et al*., 2019; Elegheert *et al*., 2017). Evidence suggests that the NLGN-MDGA2 interaction specifically inhibits the formation of excitatory synapses *in vivo* (Connor *et al*., 2016). Identification of these and other specific autism genes allowed for the development of autism mouse models.

Gene knockout mice for NRXNs, NLGNs, and MDGA2 have recently been created and all demonstrate behavioural phenotypes that bear similarities to ASD in humans. For example, in 2014, Dachtler *et al*. studied behaviour in α-neurexin II (*Nrxn2α*) knockout (KO) mice. They used a three-chambered assay for sociability, and reported that, unlike wild-type (WT) mice, *Nrxn2α* KO mice prefer spending time in the empty side of the chamber as opposed to the side with an unfamiliar mouse. In addition to deficits in social behaviour, they also noted increased anxiety, as assessed by spending more time at the periphery of an open field than WT mice. Additionally, a separate study by Grayton *et al*. (2013) found that α-neurexin I (*Nrxn1α*) KO mice also display social deficits, as assessed by a similar three-chamber method, and anxiety-like behaviours, assessed using an elevated plus maze test. ASD phenotypes have been observed in neuroligin-3 (*Nlgn3*) deficient mice as well; a 2009 study by Radyushkin *et al*. demonstrated that *Nlgn3* KO mice have reduced vocalizations and altered social memory. Furthermore, a study by Connor *et al*. (2016) found that happloinsufficient $Mdga2^{+/-}$ mice display several phenotypic ASD traits including repetitive motions, reduced social interaction, elevated E/I ratio, and long-term memory impairments. Taken together, the findings from genome-wide scans and subsequent mouse models indicate that synapse organization proteins likely play an important role in the etiology of this disorder.

Mutation of autism-susceptibility genes are thought to lead not only to synapse disorganization, but also to the disruption of certain types of synaptic plasticity, including LTP and LTD. Electrophysiological studies for LTP have been conducted in hippocampal brain slices of $Mdga2^{+/-}$ mice, demonstrating enhanced E-LTP and impaired L-LTP (Connor *et al*., 2016). Alterations in LTP coincided with memory deficits, where $Mdga2^{+/-}$ mice took a significantly longer time to re-find a previously identified hidden platform in water (Morris Water Maze)

compared to WT mice. Furthermore, in a contextual fear conditioning task, *Mdga2*$^{+/-}$ mice appeared to forget that a certain chamber elicited a foot-shock, as assessed by less freezing behaviour than WT when put back into the environment where a previous shock had been given (Connor *et al*., 2016). Many other genetic mouse models of autism also demonstrate altered synaptic plasticity. For example, a 2018 study by Letellier *et al*. found that a single point mutation in NLGN1 (Y782A/F) results in severe impairment of LTP in mice hippocampal brain slices; a study by Takeuchi *et al*. (2013) found disrupted LTP and LTD in a phosphatase and tension (PTEN) mouse model of autism; a 2010 study by Bozdagi *et al*. found impaired LTP, but unaltered LTD in a SHANK3 (SH3 and multiple ankyrin repeat domains 3) mouse model of autism; and a 2019 study by Shin *et al*. found that mice deficient for autism-implicated gene *Scn2a* display supressed LTP, but normal LTD. These are just a few of the many notable studies that have shown altered LTP and/or LTD in mouse models of autism. Thus, it is well established that certain genes have a role in autism, and many of these genes have a negative impact on LTP and LTD, corresponding to learning and memory impairments. Although numerous studies have focused on identifying synaptic plasticity aberrations in genetically altered mouse models of autism, few have devised methods for actual restoration of these deficits. An important question is raised from these studies – might it be possible to reverse LTP-LTD deficits in ASD using novel plasticity-based treatments?

1.4 Plasticity-based therapeutics for autism

Currently, plasticity-based therapeutics for autism are unavailable, but there is growing interest in this field of research. The strong evidence supporting LTP-LTD impairments and E/I ratio imbalances in ASD has led to the theory that perhaps other forms of plasticity can be used to restore these deficits. For example, there is another type of synaptic plasticity, known as

"homeostatic scaling" that could potentially be utilized to this end. Homeostatic scaling was first discovered in 1998 by neuroscientist Gina Turrigiano and her research group. They discovered that when neurons are silenced for 2 days, there is subsequent overall heightened excitability once the activity-blockade is removed (homeostatic upscaling). They also found that when neurons are chemically induced to be excessively active for 2 days, there is subsequent heightened inhibition of activity once the stimulation is removed (homeostatic downscaling) (Turrigiano *et al*., 1998). Homeostatic scaling appears to be a promising method for raising or lowering overall excitation within the brain, and, in the case of ASD where the brain is often over-excited, this may prove to be a useful therapy. Furthermore, if synaptic over-excitation is the cause of impaired LTP and LTD in autism, homeostatic scaling could potentially be utilized to improve these deficits, resulting in the restoration of learning and memory as well. These possibilities remain as open questions.

1.5 Historical summary

In summary, many historical developments have led to the intersection of synaptic plasticity and ASD, an important reference point for future therapeutic intervention. From its first description by J.M.G Itard and Leo Kanner in the late 19th and early 20th centuries, autism appeared to be a disorder characterized by mis-wiring of the brain. This was supported by morphological studies which revealed marked differences in neuronal organization and number. Early on, genetics were thought to have a significant role in this disorder, and eventually twin studies confirmed the influence of genetic heritability. The specific genes involved were identified in the 1990s and 2000s, implicating the contribution of a number of synapse organizing proteins. With the advent of genetically modified mouse models of autism, specific studies could be conducted to examine LTP and LTD deficits in conjunction with certain genetic mutations. Findings support that many

of the autism-susceptibility genes have a crucial role in synaptic plasticity, suggesting that autism may primarily be the result of aberrant synaptic changes. If this is the case, perhaps treatments would be most effective if targeted toward the restoration of known synaptic inefficiencies, such as LTP-LTD deficits, and E/I ratio imbalances. Independent developments in the field of synaptic plasticity, such as the discovery of homeostatic scaling, provide new avenues by which plasticity-based therapeutics can be explored. Continued research in ASD synaptic pathology has great potential to improve the lives of millions impacted by this disorder.

1.6 Overview of the hippocampus

The human hippocampus is a brain structure located in the medial temporal lobe. Each hemisphere of the brain contains one of two hippocampi, seated generally in the area above the brainstem and below the thalamus. The hippocampus is part of the limbic system, a group of brain structures, including the hypothalamus, amygdala, thalamus, and hippocampus, that work together to control emotion (Rajmohan & Mohandas, 2007). The shape of the hippocampus is curled resembling a ram's horn, which is why some of its anatomical regions are referred to presently as *cornu ammonis* (CA) 1, 2, and 3. "Cornu ammonis" is Latin for "ram horn," and was the original name of the structure as a whole. The name was later changed to "hippocampus" after the fish genus for seahorses, as it also resembles the body shape of this category of fish (Andersen *et al*., 2006). The hippocampal formation consists of a number of different regions including the hippocampus proper, dentate gyrus, entorhinal cortex, and subiculum. The connections between the various locations within the hippocampal formation form specific pathways. For example, neural projections from the entorhinal cortex to the dentate gyrus and CA3 form the perforant pathway; projections from the dentate gyrus to CA3 form the mossy fiber pathway; and projections from the CA3 to CA1 form the Schaffer collateral pathway

(Andersen *et al*., 2006). The types of neurons also differ depending on the hippocampal region. The dentate gyrus is composed primarily of granule cells, while the hippocampus proper is comprised mainly of pyramidal cells. Pyramidal neurons are characterized by a pyramid-shaped soma and extensive branching at the apical and basal dendrites, whereas granule cells have a more rounded cell body, and are typically smaller than pyramidal cells (Johns, 2014). The hippocampus is present in other vertebrates, including fish, reptiles, birds, and mammals (Allen & Fortin, 2013). It retains a similar structure across species and serves a critical role in spatial memory. Cells specific for encoding cognitive maps – spatial relations among objects or landmarks in the external world – were discovered within the hippocampus proper and entorhinal cortex. Place cells are a type of pyramidal cell in the hippocampus proper that demonstrate heightened activity in a specific environmental location. Using implanted electrodes to measure single-unit activity in the rat hippocampus, John O'Keefe and Jonathan Dostrovsky (1971) observed that place cells were only active when the rat was pushed and restrained by hand to particular locations in a boxed environment. In 2005, an additional location-specific cell was discovered – the grid cell. Hafting *et al*. (2005) observed that certain cells in the rat entorhinal cortex fire in accordance with a triangular lattice pattern traversing the ground plane of a circular enclosure. In their experiment, live rats were implanted with tetrodes in the dorsocaudal medial entorhinal cortex (dMEC) to record neuronal firing from multiple cells as the rats freely explored a flat, 2-meter diameter environment. The firing pattern of some cells coincided with the vertices of a 2-dimensional triangular lattice on the ground of the space explored. The researchers called these cells *grid cells,* owing to the dependence of neuronal firing on grid placement in the external environment. In addition to encoding spatial relations, the hippocampal formation is essential for creating new memories about facts and events (declarative or explicit memories).

The case of patient Henry Molaison (H.M.) highlights the function of the hippocampus in declarative/explicit memory, rather than procedural/implicit memory. At age 27, H.M. suffered severe seizures that were thought to stem from brain trauma caused by a bicycle accident at age 7 (Squire, 2009). H.M. underwent experimental surgery to alleviate the seizures, having large portions of his medial temporal lobes removed (bilateral medial temporal-lobe resection), including the amygdala and hippocampus in both hemispheres of the brain (Scoville & Milner, 1954). Although the surgery lessened the severity of his seizures, H.M. was left with the inability to form new memories (anterograde amnesia). For example, it was observed that he could only remember new facts and events for about 30 seconds. In contrast, he could easily recall events from his early life; however, he experienced some loss of previous memories (retrograde amnesia) that worsened leading up to 1-2 years before the surgical procedure. The amnesic effects severely impacted H.M.'s ability to lead a normal life, and he was dependent upon assisted living until his death in 2008 at age 82. He described his ongoing state of mind as like "waking from a dream," where the present moment is clear, but what happened just before is unknown (Milner *et al*., 1968). Interestingly, H.M. was able to learn new implicit, procedural tasks, such as how to use a walker, and improved on experimental motor skill-learning tasks (Shah *et al*., 2014). This finding implied that there are different types of memories encoded by different parts of the brain, and that the hippocampus in particular enables long-term storage of declarative memories, but is not responsible for unconscious motor learning. Similar memory deficits have been noted in other cases of hippocampal ablation in humans. For example, in the 1960s when hippocampectomy was performed on a number of cancer patients as a last resort for pain relief, many of these patients experienced anterograde amnesia following removal of the hippocampus (Gol & Faibish, 1967). In summary, the hippocampus has a vital role in the

formation of declarative memories and spatial navigation. It houses a complex system of neuronal pathways that communicate within the limbic system, and with brain structures beyond, to convert snapshots of the present moment into long-term memories and cognitive maps.

1.7 Overview of the C57BL/6 mouse

The C57BL/6 mouse is one of the most commonly used strains for research on medical diseases and disorders. It is an inbred strain originating from a colony bred by Abbie E. C. Lathrop in the early 1900s in Granby, Maryland. Lathrop provided "mouse #57" to Clarence Cook Little, who founded Jackson Laboratory, a facility that produces many different types of mice for scientific research purposes. Little bred from mouse 57 an all-black strain of identical mice, known as the C57BL/6J strain (Steensma *et al*., 2010). Due to genetic drift, there are now different substrains. For example, in the 1950s, Jackson Laboratory sent mice to the National Institutes of Health, and after many generations, this formed the new substrain C57BL/6N. The 6N and 6J substrains have notable differences in traits related to pain sensitivity, ethanol consumption, and fear learning (Bryant, 2011). A study by Fertan *et al*. (2020) found that behavioural traits of the *Mdga2*$^{+/-}$ mouse model of ASD vary depending on the background substrain used, where the C57BL/6N performed better than C57BL/6J on tasks measuring visual ability and learning. Thus, it is important when conducting research with C57BL/6 mice to take into account the substrain used. Appearance-wise, the C57BL/6 mouse has a dark brown fur coat, which almost appears black, and can have small patches of white, typically behind the ears. Behaviour-wise, the C57BL/6 mouse can be distinguished from other strains by its extensive tendency to "barber." Barbering refers to the action of one mouse plucking fur from another, resulting in bald patches. It is thought to be an indication of social hierarchy, where the more dominant mice "barber" the less dominant (Kalueff *et al*., 2006). C57BL/6 mice also have unique temperament traits that

distinguish them from other widely used inbred strains of lab mice, such as the BALB/c. In a study by Sultana *et al*. (2019), C57BL/6 mice were found to demonstrate heightened propensity for exploration. There is also evidence that C57BL/6 mice have higher levels of empathy compared to the BALB/c strain (Chen *et al*., 2009). The C57BL/6 mice also exhibit less hierarchical-based aggression; a study by Bisazza *et al*. (1981) showed that C57BL/6 male mice were less territorial and aggressive towards each other than the BALB/c strain. The development of unique morphological and behavioural features of the C57BL/6 mouse was facilitated by human influence, through evolutionary commensal relationships and selective breeding for certain traits.

The C57BL/6 strain has provided a means for many important breakthroughs in scientific research. For example, they have been used to discover genes for human deafness (Bryda, 2013), and for the development of chemotherapy and HIV treatments (DeVita & Chu, 2008; Marsden, 2020). Through manipulation of genes and environment, they have also been useful as models for neurodevelopmental and neurodegenerative disorders, including autism, schizophrenia, Alzheimer's disease and fragile X syndrome. For example, by using an *Fmr1*-KO C57BL/6 mouse to study synaptic plasticity in fragile X syndrome, Huber *et al*. (2002) discovered that FMRP has a functional role in regulating long-term depression, which has led to new ideas for therapeutic approaches to this disorder (Bear, 2005). Mice in general are helpful in medical research because of their genetic similarities to humans. Many of the genes implicated in human neurological conditions are also found in mice, where similar mutations between mice and humans cause similar phenotypes. Additionally, because mice have a relatively short lifespan (~2 years) and produce high volumes of offspring, scientists can study developmental disorders in

mice at an accelerated pace. Lastly, mice are relatively cheap and easy to maintain, costing about $1 per day to be cared for in an animal care facility. Use of the C57BL/6 mouse further enhances the utility of mice because it provides a stable genetic background for experiments; when different labs are using the same common inbred strains, cross-study analysis and interpretation can be accomplished with higher accuracy.

Figure 1.7: A curious, juvenile C57BL/6 mouse.

1.8 Objectives and hypotheses

The objective of this thesis is to explore synaptic plasticity in autism spectrum disorder through the use of electrophysiology techniques and autism mouse models. Note that due to the pandemic, the original ASD model mouse, *Mdga2*$^{+/-}$ was not available. In collaboration with Dr. Crawford's group, I switched to an alternative, idiopathic autism model (PGE_2). My first hypothesis is that hippocampal synaptic plasticity in the PGE_2 mouse model of autism is impaired (discussed in chapter 3). My second hypothesis is that homeostatic scaling can restore synaptic plasticity deficits in autism mouse models (discussed in chapter 4).

CHAPTER 2: ASSEMBLY OF ELECTROPHYSIOLOGY EQUIPMENT

2.1 INTRODUCTION

2.1.1 Mouse hippocampal slice recording

Before any hypotheses can be tested, it is essential that proper equipment is assembled and working methods are devised. Investigating LTP in autism mouse models is not possible unless baseline field excitatory post-synaptic potentials (fEPSPs) are able to be seen within the recording system of choice. fEPSPs are extracellularly recorded excitatory post-synaptic potentials (EPSPs) that capture responses from a population of neurons. In the mouse hippocampal CA1 region, fEPSP waveforms have different shapes depending on whether recording took place at the cell bodies or the dendrites. In stratum pyramidale (cell body layer), fEPSPs are upward-deflected, whereas in stratum radiatum (dendritic region), fEPSPs are downward-deflected (Sweatt, 2009). There are three main components to a fEPSP waveform, namely, the stimulus artefact, fibre volley, and population EPSP. The stimulus artefact is a result of the stimulus itself, the fibre volley is the signal from the pre-synaptic action potentials, and the EPSP arises from the activation of the post-synaptic neurons. Most LTP studies utilize rodent hippocampal slices, as this form of experimental substrate offers retained synaptic circuits and easy accessibility for electrophysiological recording (Lein *et al*., 2011). Furthermore, rodents are simple to maintain in the laboratory, and many features of the rodent hippocampus are applicable to humans as well. However, fEPSPs have been successfully recorded in many other classes of animals including primates, fish, reptiles, and insects.

2.1.2 Cricket cercal system as an alternative model

Although mouse hippocampal slices are ideal for studying LTP, they may not be the most efficient material for use in troubleshooting equipment set-up. For example, when testing if electrophysiology equipment can pick up general biological signals, or when learning how to navigate new software, simpler life-forms may be better suited for the task. House crickets could potentially be a better alternative to mice in such situations, as they are cheaper, easier to maintain, and do not require as much time or resources to dissect and prepare. For instance, one cricket only costs 14 cents and, because crickets continue to respire through the sides of their body during dissection, no oxygen bubbling is required. For testing biological signal resolution, fEPSPs in crickets may provide sufficient indication of whether or not a set-up is working. fEPSPs have previously been successfully recorded from the cricket cercal system (Ogawa & Mitani, 2015). The cercal system consists of a mechanosensory processing pathway, allowing the cricket to respond appropriately to environmental stimuli. It involves distinct structures known as cerci, which are two antenna-like structures extending from the posterior end of the abdomen. The cerci are covered in fine hairs that allow the cricket to sense faint movements of surrounding air. Vibration of the mechanoreceptor hairs on the cerci propagate action potentials towards the abdomen, into the terminal (cercal) ganglion, containing cell bodies of the giant interneurons that extend anteriorly to inform responsive leg and head movements (Figure 2.1.1) (Jacobs *et al.*, 2008; Mendenhall & Murphey, 1974).

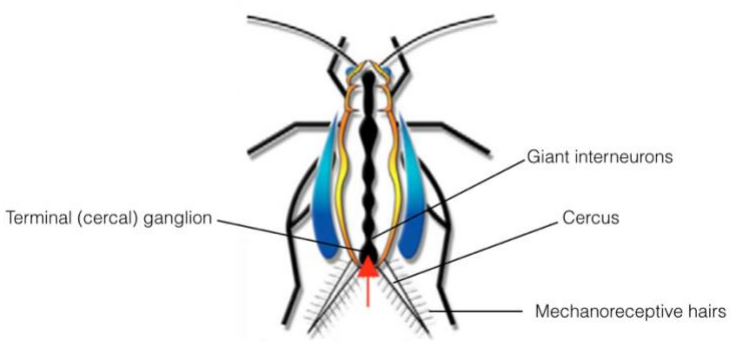

Figure 2.1.1: Structures involved in the cricket cercal sensory system. Red arrow indicates the direction of sensory information flow. Image adapted from Jacobs *et al*. (2008).

2.1.3 Electrical noise

When setting up electrophysiology equipment, one of the earliest tasks required is to eliminate as much noise as possible. Any electrical device within the vicinity of the equipment can cause interference and obstruction of the biological signal of interest. This includes nearby computer monitors, lights, power cables, electrodes, amplifiers, the preparation and digitization process itself, as well as mechanical vibrations from fans and heating devices (Molecular Devices, 2012). To ensure the highest quality of recording data, as much background noise as possible must be reduced to achieve an appropriate signal-to-noise ratio, meaning that the voltage differences generated by the object of interest are not overpowered by the voltage differences generated by other sources. Background noise consists of a number of different components, such as thermal noise, shot noise, flicker noise, and alternating current (AC) 60 Hz noise. Thermal noise is due to the property of Brownian motion present in all particles; even electrons are subject to this random fluctuation in position, which contributes to a non-uniform baseline signal. Temperature differences contribute to thermal noise, as higher temperatures exacerbate the impact of Brownian motion on charged particles. Another contributor is shot noise, which is a property of the flow of electrons as a whole, rather than the individual particles themselves. It occurs when current crosses barriers, such as PN junctions, which cause disturbances in the flow. Shot noise

can be thought of as similar to the effect of turbulence in flowing water. Flicker noise, or 1/f noise, is also a property of current, and it is most apparent at low frequency. The reason behind why flicker noise occurs is not entirely clear. It may be due to the random build up and release of charge in the circuit, or another possibility is that it may be caused by slight differences in current mobility throughout the path of motion (Chauhan *et al*., 2015). Lastly, 60 Hz noise is a product of the AC voltage fluctuations as current moves in alternating directions. It is easy to identify, as its characteristic voltage oscillation cycle occurs ~60 times per second. Taken together, all these types of noise – AC, flicker, shot, and thermal – contribute to the overall background disturbances that can be disruptive to the recording of biological signals. It is important to be aware of the causes of background noise to aid in the task of its reduction.

2.2 MATERIALS & METHODS

2.2.1 Mouse Hippocampal Slice Preparation

C57BL/6 mice were ordered from supplier Charles River and maintained at the York University animal facility, department of Biology (Toronto, ONT, Canada). Mice had continual access to food and water, and were housed at room temperature on a 12h:12h light:dark cycle. Mice were acclimatized to the facility for at least one week upon arrival before use in experiments. Juvenile and adult mice, between the ages of 5 - 26 weeks old, were sacrificed by cervical dislocation followed by decapitation. The brain was removed and rapidly cooled for ~45 seconds in ice-cold recovery solution (Table1) or aCSF (Table 2) bubbled with carbogen (95% O_2, 5% CO_2). The brain was then hemisected and hippocampi were removed from both hemispheres. Hippocampi were sliced using a manual tissue slicer to a width of 400 microns. Recovery time,

electrophysiology rig equipment, and synaptic plasticity protocols varied depending on the particular experiment.

Table 2.2.11: Recovery solution for mouse hippocampal brain slices. Ingredients added to 500mL MilliQ water and pH adjusted to 7.35 with HCl.

Component	Molarity (mM)	Molecular Weight (g/mol)	Amount for 500mL
NMDG	93	195.2	11.7 g
KCl	2.5	74.6	95 mg
NaH2PO4	1.2	138	95 mg
NaHCO3	30	84	1.05 g
Glucose	25	180.2	1.8 g
Sodium ascorbate	5	198	65 mg
Sodium pyruvate	3	110	65 mg
MgSO4.7H2O	10	246.5	700uL
CaCl2.2H2O	0.5	147	500uL
pH 7.35			
mOsm 300-310			

Table 2.2.12: Recording solution (aCSF) for mouse hippocampal brain slices. Ingredients added to 1L MilliQ water and pH adjusted to 7.35 with bubbling of carbogen.

Component	Molarity (mM)	Amount for 1L	Molecular Weight (g/mol)
NaCl	124	7.25 g	58.44
KCl	3	220 mg	74.56
CaCl2	2	1000uL	147
MgCl2	1	500uL	202
NaH2PO4	1.25	173 mg	138
NaHCO3	26	2.18 g	84
Glucose	15	2.7 g	180
pH 7.35			
mOsm 310-320			

2.2.2 Mouse hippocampal slice recording using the Kerr Tissue Recording System

After hippocampal dissection and slicing, ~10-20 slices were left undisturbed for 1 hour in a

recovery submersion chamber heated to 32°C using a general purpose water bath (Thermo Fisher Scientific, Fisherbrand™, Isotemp™). Within the recovery chamber, slices were incubated in carbogenated artificial cerebrospinal fluid (aCSF). After 1 hour at 32°C, the recovery chamber was removed from the water bath for an additional recovery period of 1 hour at room temperature (21°C). Slices were then transferred using a disposable Pasteur pipette to the Kerr Scientific Instruments (KSI) Tissue Recording System™ chamber. Extracellular recordings of field excitatory postsynaptic potentials (fEPSPs) were conducted using the recording and stimulating electrodes supplied by the KSI Tissue Recording System™. During the measuring period, a constant flow of carbogenated aCSF was maintained through the recording chamber, at a rate of 1-2mL/min. Signal information was relayed to an ADInstruments PowerLab 4/26 data acquisition device and interpreted by the computer software LabChart 8.

2.2.3 Mouse hippocampal slice recording using the Axon Instruments recording system

When recording from the Axon Instruments rig, slices were no longer incubated in a separate submersion chamber for recovery; rather, after dissection and slicing, ~10-20 slices were placed in a heated interface chamber (BSC1-2; Scientific Systems Design Inc) and allowed to recover undisturbed for 1.5 hours. The interface chamber was heated to 30°C using a PTC03 Scientific Systems Design Inc. proportional temperature control unit. The stimulating electrode was constructed from 0.002 inch nichrome wire (80% nickel/20% chromium; A-M Systems™), threaded through a 1.5mm width borosilicate glass capillary (TW150F-4; World Precision Instruments), with ends sealed using ArmorCoat™ quick setting epoxy. The stimulating electrode was connected to a DS3 Isolated Current Stimulator (Digitimer, LLC) to control the strength and duration of the electrical stimulus. The recording microelectrode was also constructed from a 1.5mm width borosilicate glass capillary (TW150F-4; World Precision

Instruments), pulled to a fine tip using a P-97 Flaming/Brown type micropipette puller. The recording electrode was backfilled with aCSF and secured to an Axon Instruments CV-7B current/voltage clamp headstage. A new recording electrode was constructed for each slice recording measurement, with an acceptable resistance of 1-3MΩ. Signal information from the recording electrode was relayed from the headstage to an Axon™ Digidata® 1550B low-noise data acquisition system with HumSilencer™, and MultiClamp™ 700B computer-controlled current and voltage clamp amplifier. Signal information was converted to readable output data using the computer software Axon™ pCLAMP™ 11. Mechanical noise reduction was achieved by using a Newport air table to support the brain slice interface chamber and surrounding equipment, including the electrode micromanipulators (M3301; World Precision Instruments) and Laxco™ LMS-Z200 Stereo Zoom microscope.

2.2.4 Cricket cercal system recording

Juvenile house crickets, *Acheta domesticus*, were obtained from a colony maintained at PetSmart (Lawrence Allen Centre, Toronto, ONT, Canada). Upon arrival at York University, crickets were housed at room temperature in a 15.5cm (length) X 8.5cm (width) X 10cm (height) portable plastic pet carrier. A maximum of 12 crickets were held in the container at one time. Crickets were maintained on a diet of fresh apple slices, provided daily for 1-2 weeks, the time span after which all crickets were used. The container was enriched with layers of cardboard egg cartons to prevent cannibalism and fighting among cagemates. Crickets were anesthetized by placement in a -20°C freezer for ~3min. Crickets were then rapidly decapitated and de-limbed on ice using fine-pointed micro-scissors. A makeshift dissection surface was constructed from a metal washer wrapped in multiple layers of Parafilm®, on which sewing pins were used to immobilize the crickets' thorax and abdomen during dissection. Crickets were dissected by cutting down the

midline of the dorsal exoskeleton and removing most of the abdominal organs (midgut, hindgut, Malpighian tubules, testes, ovaries) to access the underlying terminal ganglion. During and after dissection, cricket preparations were bathed in *Acheta* Ringer's solution (Table 2.2.4), isotonic and of similar composition to cricket circulatory fluid (hemolymph). Extracellular recordings of field excitatory postsynaptic potentials (fEPSPs) were conducted using the KSI Tissue Recording System. Signal information was relayed to an ADInstruments PowerLab 4/26 data acquisition device and interpreted by the computer software LabChart 8.

Table 2.2.4: *Acheta* Ringer's solution. Modified from Coast and Kay (1994), with $NaHCO_3$ substituted for NaOH to raise pH to ~7.2. Ingredients added to 50mL MilliQ water.

Substance	Molarity (mM)	Amount for 50mL	Molecular Weight (g/mol)
NaCl	100	0.2922 g	58.44
KCl	8.6	0.03205 g	74.55
CaCl2	2	100uL (1M stock)	N/A
MgCl2	8.5	425uL (1M stock)	N/A
NaH2PO4	4	0.02399 g	119.98
Glucose	24	0.21619 g	180.16
NaHCO3	21	0.086 g	84

2.2.5 Statistical analyses

Data analysis was conducted using Microsoft® Excel 2018 and GraphPad Prism 8.

2.3 RESULTS

2.3.1 Overview of the Kerr Tissue Recording System

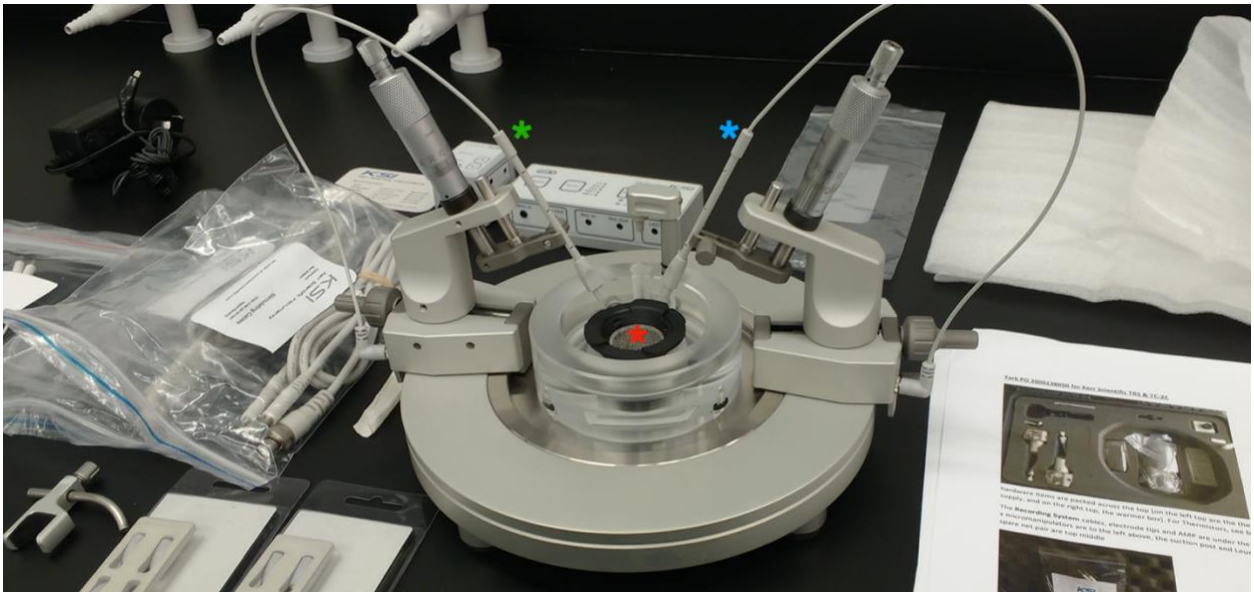

Figure 2.3.1: The Kerr Tissue Recording System™ designed to measure responses from electrically excitable tissues. Mouse brain slices can be held in the central chamber marked with a red asterisk. Electrophysiological recordings are obtained using the stimulating and recording electrodes, indicated with blue and green asterisks, respectively.

Setting up proper equipment is the first step to obtaining reliable electrophysiological recordings. The first rig I attempted to set up was the Kerr Scientific Instruments (KSI) portable rig, known as the Kerr Tissue Recording System™ (Figure 2.3.1). This rig is innovative because it takes up less space and can be assembled and taken apart with ease, compared to other brain slice recording set-ups. However, obtaining reliable recordings from the Kerr Tissue Recording System™ proved to be difficult.

2.3.2 Troubleshooting the Kerr Tissue Recording System with mouse brain slices

The KSI guidelines for equipment set-up recommend placing mouse brain slices between the chamber base and mesh top net for optimal recording (Kerr, 2009). Following these guidelines,

the top net was found to deform and lose shape leading to movement and damage of the slices within the chamber. To optimize recording from this system, I tried alternative techniques for slice placement. Some of the various methods included recording from slices resting above the top net (Figure 2.3.21B), and under weighted paperclips (Figure 2.3.21C). Waveforms obtained in all methods did not appear as stereotypical fEPSPs (Figure 2.3.22); although some resembled the general shape, all were missing the characteristic presynaptic fibre volley.

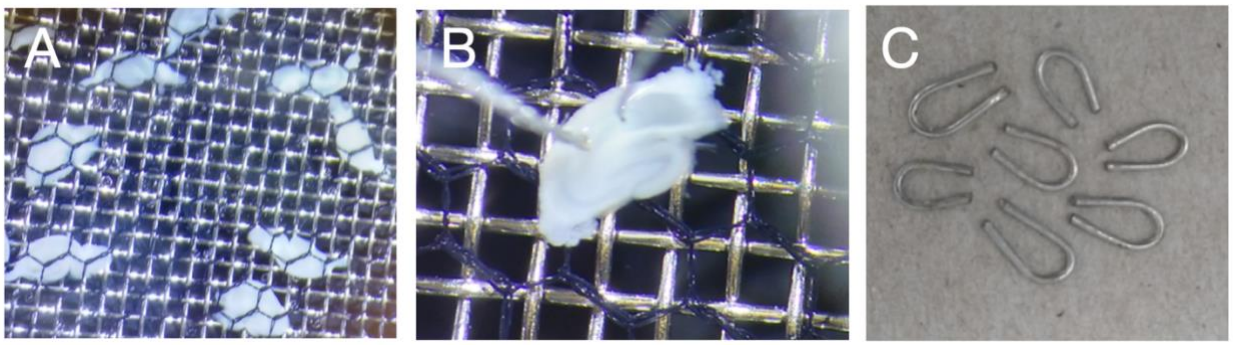

Figure 2.3.21: Optimization of hippocampal slice preparation within the KSI Tissue Recording System. A number of slice placement techniques were used, including A) the recommended placement of slices between the metal base and top net (black wire mesh), B) recording from slices resting above the top net, and C) using paperclips that were cut and bent to hold the hippocampal slices, as a replacement for using a top net.

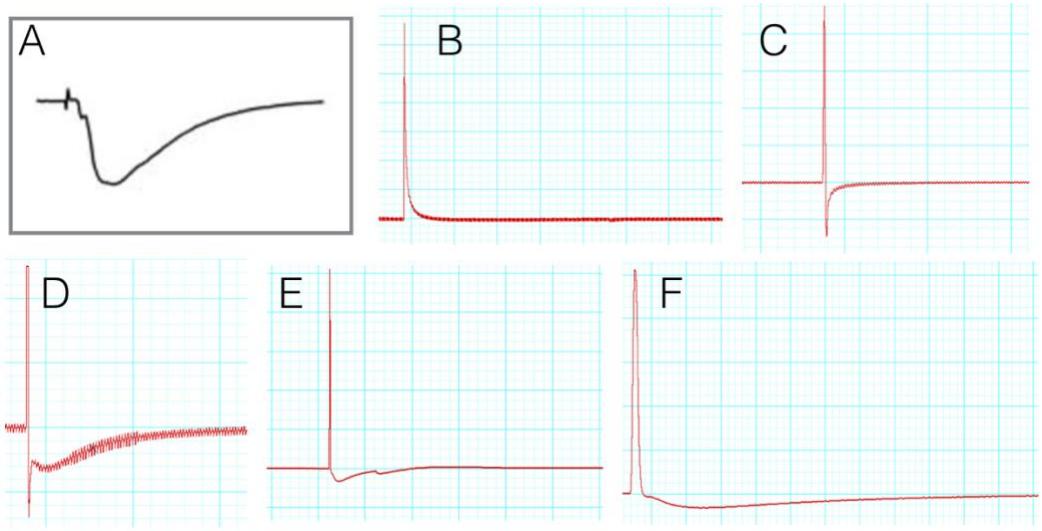

Figure 2.3.22: Waveforms obtained using the KSI Tissue Recording System lacked signature fEPSP features. A) Represents a real fEPSP obtained in an outside study by Mlinar *et*

al. (2008). B & C) The appearance of the stimulus artefact during KSI recording was variable. D, E, & F) Representative examples of suspected hippocampal fEPSPs obtained using the KSI rig; however, whether these are truly fEPSPs remains unknown because they lack visible presynaptic fiber volleys.

The use of mice for ongoing troubleshooting of equipment may not be necessary. The Canadian Council on Animal Care (CCAC) recommends replacement of sentient life forms (e.g. mice) where possible with non-living substitutes or species with lower potential for pain perception (CCAC, 2019). In following these guidelines, I decided to replace the use of mice for crickets in further troubleshooting experiments.

2.3.3 KSI troubleshooting with crickets

The use of crickets within the KSI Tissue Recording System was explored as a less costly and ethical alternative to using mice for troubleshooting purposes. A number of cricket dissection methods were attempted, with the best method proving to be from the dorsal side with abdominal organs removed (Figure 2.3.31). Recording of fEPSPs from the cercal ganglion yielded mixed results, with a variety of waveforms created (Figure 2.3.32).

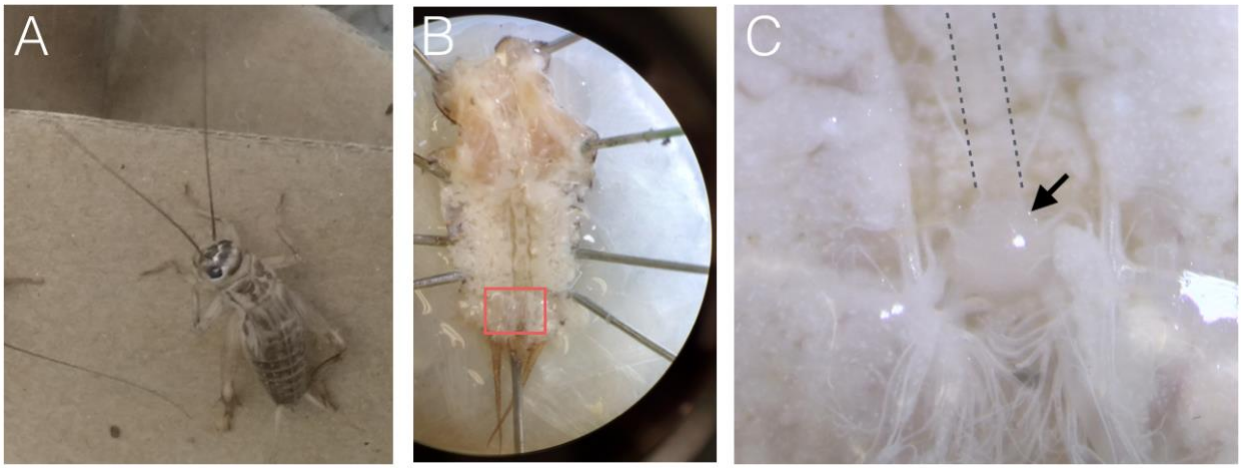

Figure 2.3.31: Method of cricket dissection to access the cercal ganglion. A) Live juvenile cricket obtained from PetSmart. B) Dissected cricket opened from the dorsal side, with internal organs removed. Red box indicates the area of interest. C) Close-up of exposed terminal cercal ganglion (circular mass of tissue indicated by black arrow). Lower giant interneurons can also be

accessed by this method; dotted lines highlight the path of giant interneurons (translucent) extending from the cercal ganglion.

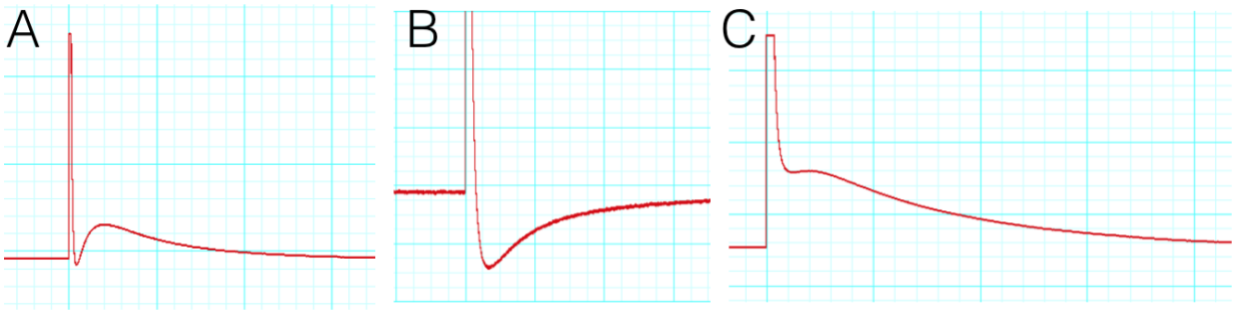

Figure 2.3.32: Representative examples of potential cercal ganglion fEPSPs. The waveforms adopted a variety of shapes shown in A, B, and C. Whether these are truly fEPSPs remains unknown due to lack of visible presynaptic fiber volleys.

Although some waveforms appeared to be fEPSPs, the missing presynaptic fiber volleys indicated that the KSI system was still not quite optimized for reliable electrophysiological recordings.

2.3.4 KSI troubleshooting with electrical noise reduction

The inability to obtain consistent and distinct hippocampal fEPSPs led to an in-depth investigation into the factors affecting resolution of electrophysiological measurements. All equipment was taken apart and reassembled to determine if certain components were causing excessive background noise. One lamp, in particular, was found to be an unusually high source of background noise (Figure 2.3.41 A, B, C). Additionally, set-up in an isolated room with a Faraday cage helped to further reduce much of the background noise (Figure 2.3.41 D, E, F). Upon reassembly, the minimum background noise possible covered a range of 10-14 mV (Figure 2.3.42). Since no further equipment could be removed without compromising the essential components, the next step was to investigate if recording solution could be optimized to reduce noise. The concentration of recording solution was found to have a dramatic impact on background noise, where lower concentrations promoted an increase in random noise (Figure

2.3.43). Furthermore, higher volume of the recording solution appeared to increase noise, but only at low solute concentration (Figure 2.3.44). Background recording was strongly affected by solution concentration and volume, leading to the idea that perhaps the properties of a stimulus would also be dependent on these same factors. Stimulus artefact strength was found to be altered by solution concentration and volume (Figure 2.3.45). The stimulus strength, as measured by the change in voltage of the artefact (Figure 2.3.45A), significantly increased with higher solution concentration as well as with lowered solution volume (Figure 2.3.45B). A significant interaction effect was also observed between solution concentration and volume on stimulus strength.

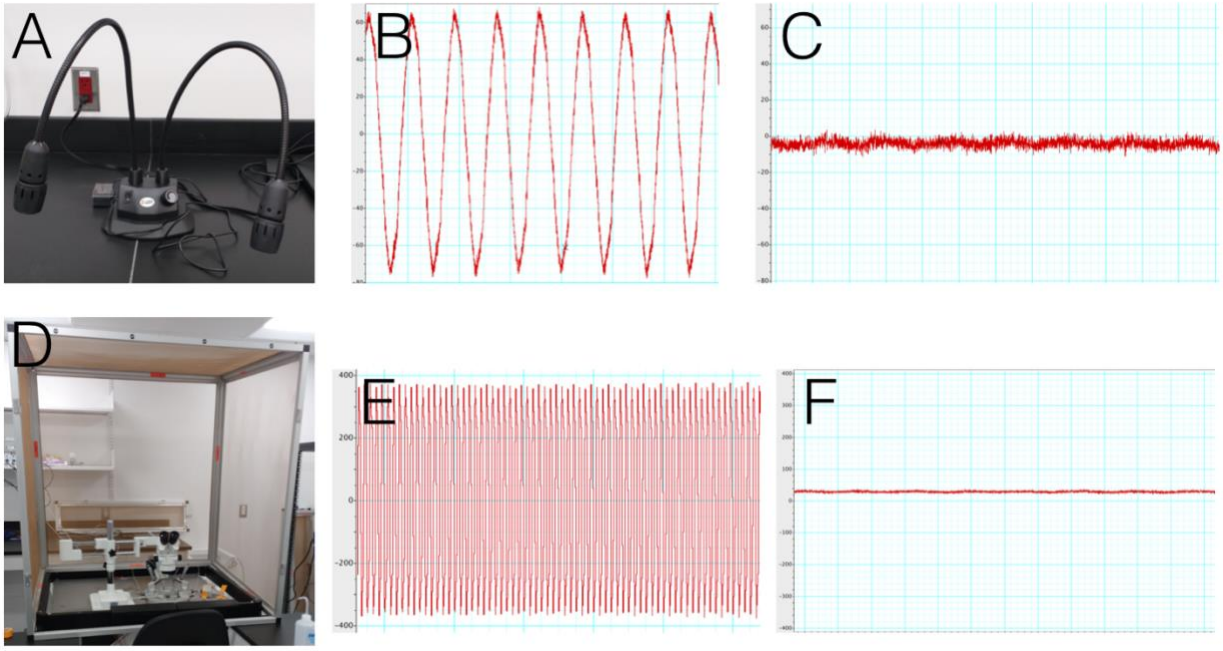

Figure 2.3.41: Background noise was greatly reduced by shielding and removal of adjacent electrical devices. One particular lighting device (A) caused a large amount of interference (B), which was evident in the noise reduction (C) that occurred upon its removal. Setting up equipment in an isolated room with Faraday cage (D) also resulted in strong reduction of background noise (F) in comparison to set-up in the larger main room with no Faraday cage (E). Y-axis scaling for representative noise data is the same for B and C (+60 mV to -80 mV), and for E and F (400 mV to -400 mV).

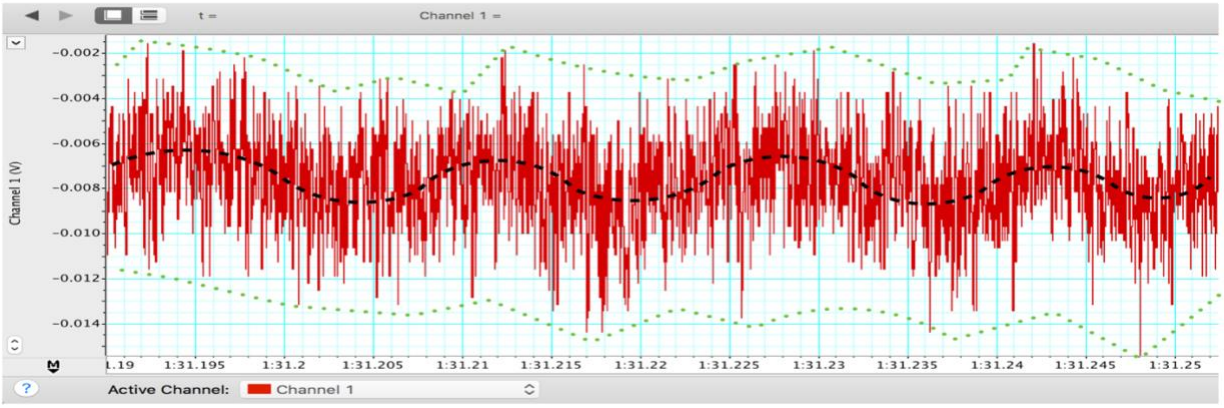

Figure 2.3.42: The lowest noise level achieved had a range of 10-14 mV. Black dotted line indicates the AC 60 Hz frequency. Green dotted line borders the additional width of the signal, likely comprising thermal, shot, and flicker noise. Voltage data was collected at the highest resolution available; 100,000 samples per second, amplified with 250X gain.

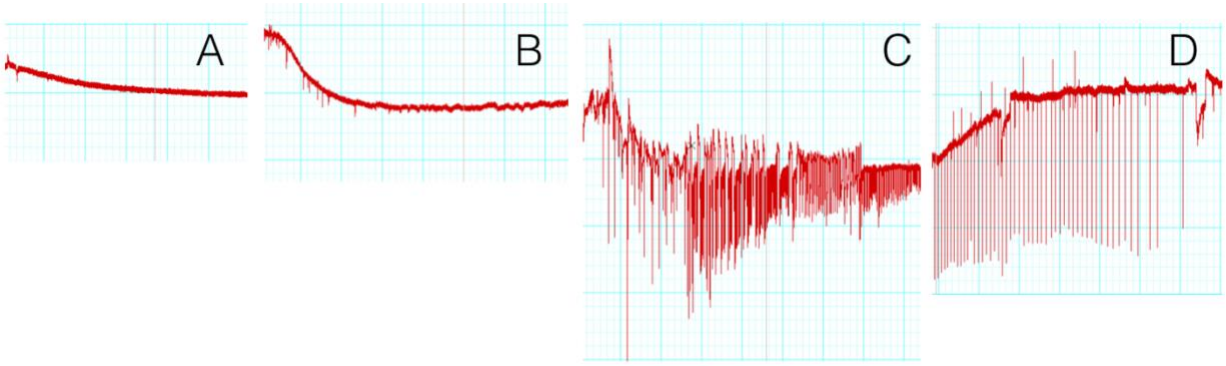

Figure 2.3.43: Background noise increased with decreasing solution concentration. NaCl concentration in surrounding solution was reduced in the following order: 1M, 0.1M, 0.01M, 0M (pure water). Corresponding background noise is shown in A, B, C, and D, respectively.

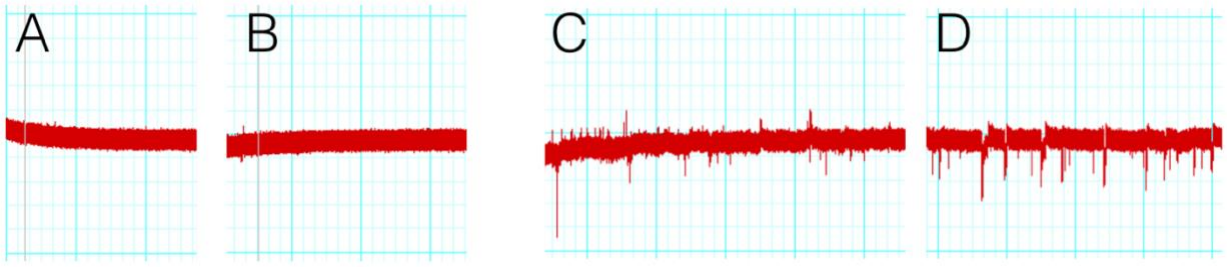

Figure 2.3.44: Background noise increased with solution volume only at low concentration. When NaCl concentration was high (1M; A, B), volume of surrounding solution had no effect on background noise (A, low volume; B, high volume). However, at low concentration (0.01M; C, D) background noise increased with surrounding solution volume (C, low volume; D, high volume).

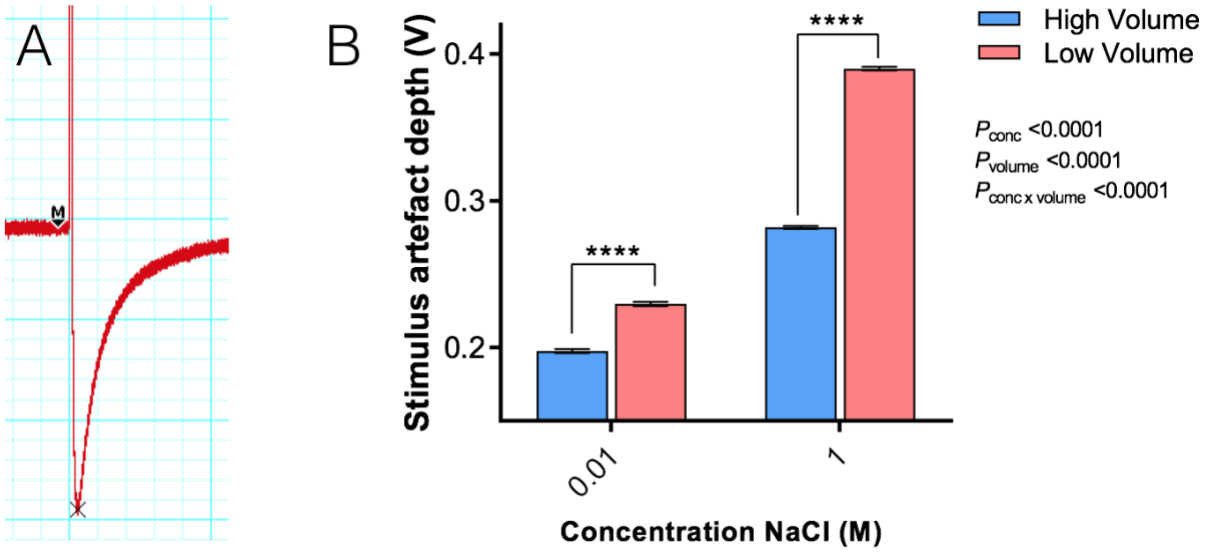

Figure 2.3.45: Stimulus artefact strength is altered by solution concentration and volume. Constant stimulus was applied every 4 seconds (1.5 V strength, 0.001 pulse width), and depth of the stimulus artefact was measured (A) as change in voltage from the marker ("M" with black arrow) to the cross symbol at the lowest point. Stimulus artefacts in high and low NaCl concentration and volume, were measured and analyzed (B). Data represent means ± SEM for *n*=10 per group. Asterisks indicate a significant difference within concentration groups, assessed by Tukey's multiple comparison test (P <0.0001). Embedded P-values denote concentration, volume, and interaction effects assessed by two-way ANOVA using GraphPad Prism 8 software.

Despite reduction of noise and gaining a better understanding of the parameters that may be affecting noise levels, no definitive fEPSPs could be observed in either mice or crickets. The question still remained – are these observed waveforms real biological responses?

2.3.5 Defining low resolution fEPSP responses using the KSI system

An experiment was designed to determine with higher certainty whether the waveforms observed using the KSI rig were real biological signals. This experiment compared the waveform amplitudes obtained from hippocampal mouse slices to the waveform amplitudes obtained in the surrounding saline. It was found that the response amplitude increased with increasing stimulus intensity only when measuring from biological tissue (brain slices) and not from the peripheral

saline (Figure 2.3.51). Response amplitude became significantly greater in the brain slices at stimulus intensity 5V and upwards, as assessed by Bonferroni's multiple comparisons test. The response curves showed visibly distinct features when obtained from tissue slices (Figure 2.3.51B) compared to the saline-only condition (Figure 2.3.51C). Waveforms from slices demonstrated a downward deflection below baseline immediately following stimulation, which is characteristic of fEPSPs. In contrast, the waveforms obtained from the peripheral saline showed no shift in voltage following stimulus artefact.

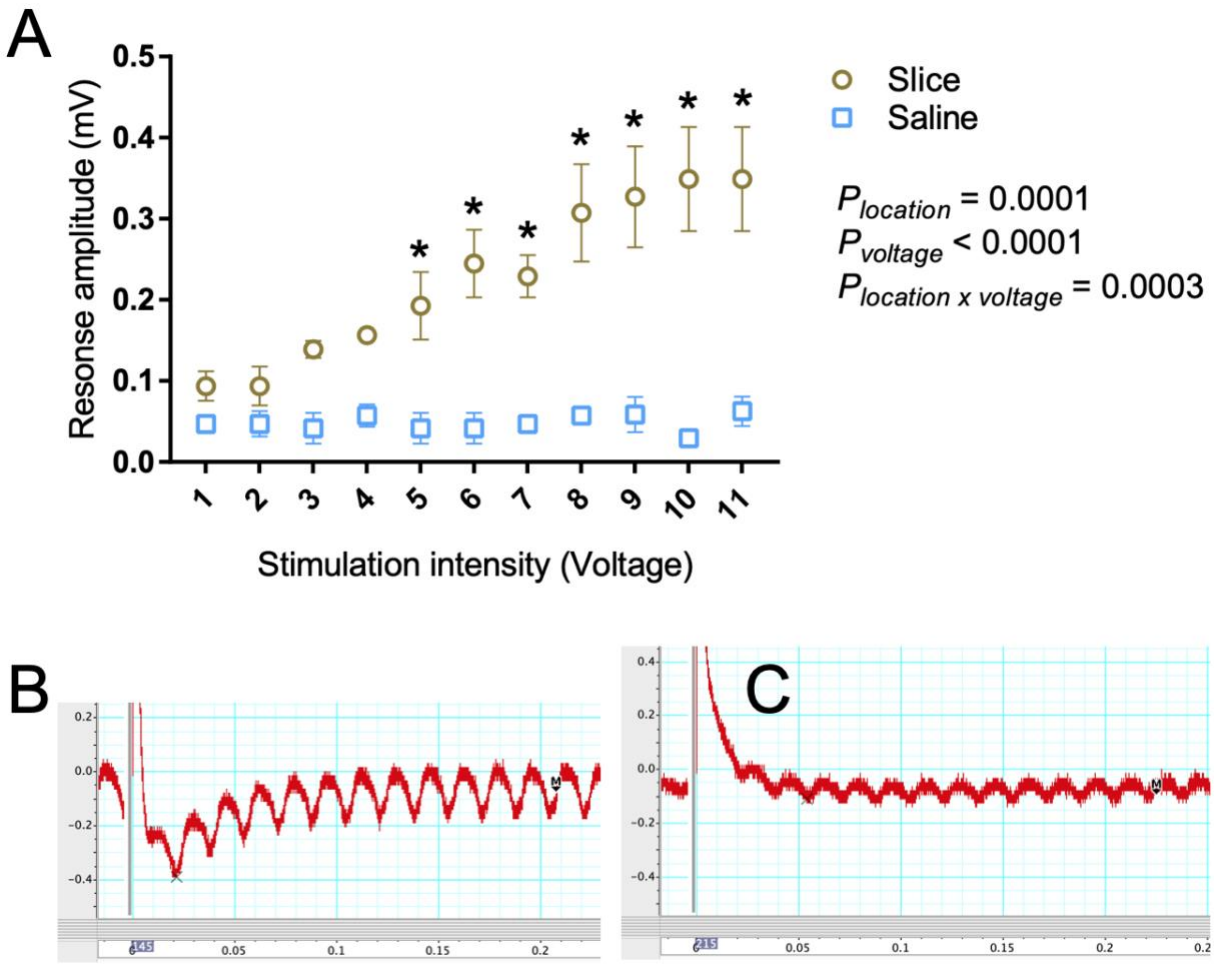

Figure 2.3.51: Voltage-dependent increase in response amplitude serves as evidence for fEPSPs generated using the KSI portable rig. A) Response amplitude increased with

increasing stimulation intensity only when recordings were taken from the CA3-CA1 region of hippocampal slices. No voltage-dependent change in response amplitude was observed when recording in the absence of slices (recording in aCSF only). n=3 slices for the slice location group, and n=3 separate locations in saline for the saline group. All slices were obtained from one mouse. There were significant effects of location (slice versus saline, $P = 0.0001$), voltage ($P < 0.0001$), and interaction between location and voltage ($P = 0.0003$), as assessed by two-way ANOVA. Asterisks indicate a significant difference ($P < 0.05$) between slice and saline groups at a particular stimulation intensity, as assessed by Bonferroni's multiple comparisons test. B) A representative trace in LabChart depicting a potential fEPSP elicited from an 11V stimulus in a hippocampal slice. Recordings were taken at 250x gain with 100k/s sampling resolution. C) A representative trace depicting a response to an 11V stimulus in the absence of a hippocampal slice (saline only). Response amplitude was measured as the difference between the midpoint of the noise near time 0.2 seconds after stimulus (indicated by the marker 'M') and the lowest point following stimulus within 0.06 seconds (indicated by the cross)

Although this provided evidence that fEPSPs can be measured using the KSI rig, the resolution was still suboptimal. The visibility of the presynaptic fiber volley is an important indicator of slice health and field measurement consistency. Since to date no presynaptic fiber volley has been observed using the KSI system, this set-up in its current state is unable to provide the waveform refinement needed to ensure accuracy.

2.3.6 Overview of the Axon Instruments recording system

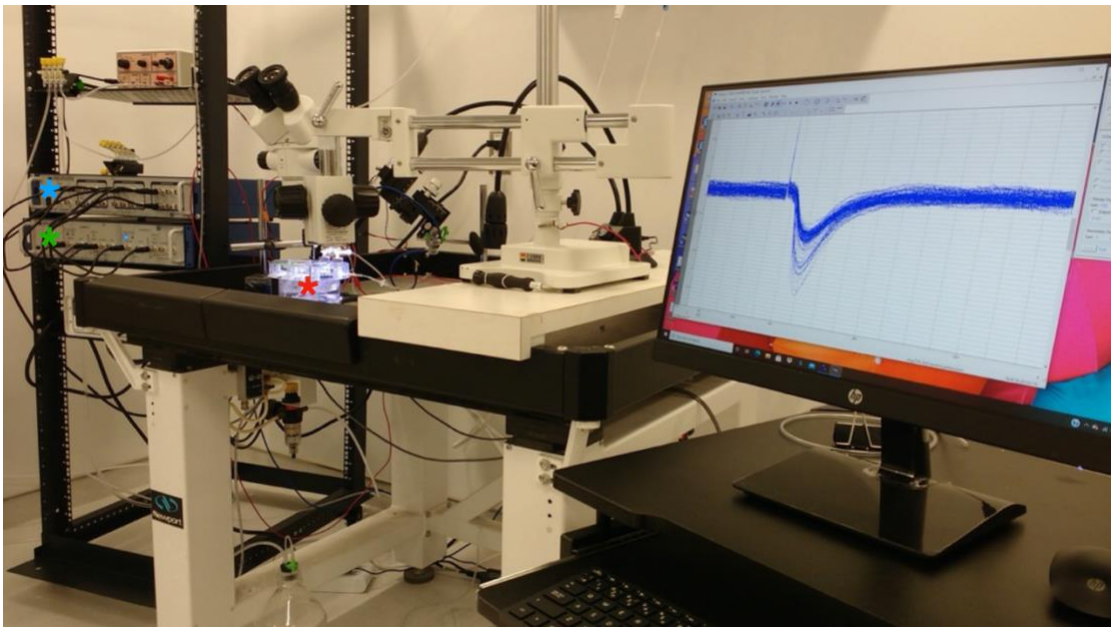

Figure 2.3.6: The Axon Instruments non-portable rig. Mouse brain slices are placed in the interface chamber, marked with a red asterisk. Voltage responses from biological tissue are translated into measurable waveforms using the Axon Instruments digitizer (blue asterisk) and amplifier (green asterisk).

Another rig by Axon Instruments was available for measuring fEPSPs (Figure 2.3.6). Since extensive troubleshooting with the KSI portable rig did not yield recordings of high enough resolution, I decided to try using this new Axon Instruments set-up.

2.3.7 Reduction of electrical noise by grounding

The initial recordings from the Axon Instruments rig revealed only patterns of electrical noise (Figure 2.3.7A). To eliminate this noise, all components of the rig were grounded. Grounding wires were fixed to any ungrounded components and this reduced the noise level significantly, leading to fEPSP recordings with high enough resolution to visibly see the presynaptic fiber volley (Figure 2.3.7B). With successful recording of baseline fEPSPs, the next step was to test if long-term potentiation (LTP) could be induced.

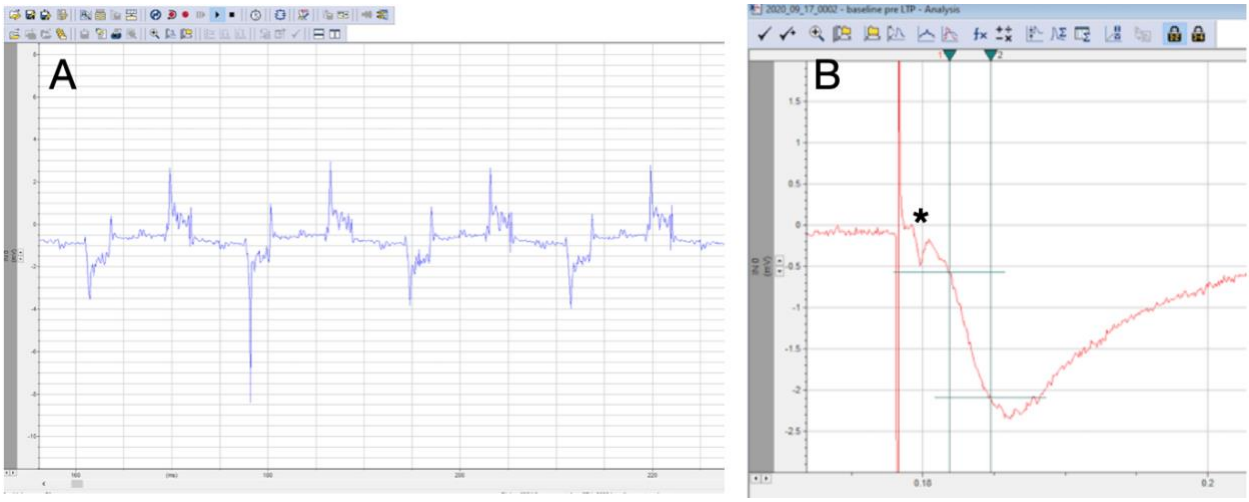

Figure 2.3.7: The effect of grounding on fEPSP recordings from the Axon Instruments rig. A) In the absence of grounding wires, the electrical noise overpowered the biological signal. B) A healthy hippocampal slice fEPSP visible only after applying grounding wires to all parts of the rig. The presynaptic fiber volley is indicated with a black asterisk.

2.3.8 Troubleshooting LTP Induction

To induce LTP, baseline recordings were taken for 20 minutes with 1 single-pulse stimulation applied per minute, and then 1 x 100 Hz stimulation was applied. Comparison of baseline responses before and after the 1 x 100 Hz stimulation demonstrated that LTP induction was possible using the Axon Instruments rig. Figure 2.3.81 displays the first 6 attempts at LTP induction. It was apparent from all experiments that after high-frequency stimulation (HFS), the slope of the fEPSPs increased; however, the decay of this increase was inconsistent among the various trials. For trial A, C, and E (Figure 2.3.81 A, C, & E) the slope of the fEPSPs continued to increase after HFS. The baseline recordings, between time 0-20 minutes, in trial A also showed a trend of increasing slope. In trial B, D, and F (Figure 2.3.81 B, D, & F) the slope of the fEPSPs continually decreased after HFS to levels below baseline. The baseline slopes also demonstrated a downward trend. In trial B, the slope abruptly dropped to zero after time ~40 minutes. This was likely due to stimulator battery depletion which occurred during another trial, where the effect of stimulator battery strength was tested (Figure 2.3.82). It was found that having low battery charge in the stimulator results in a downward trend of fEPSP slopes both during baseline recording and after HFS (see Figure 2.3.82 time 0-50 minutes). This downward trend eventually led to a sharp drop of slope levels to zero (Figure 2.3.82 time 50-65 minutes). To investigate if stimulator batteries were the source of this effect, I switched the old batteries for newly charged ones and the slope recordings returned back to heightened levels (Figure 2.3.82 time 70 minutes).

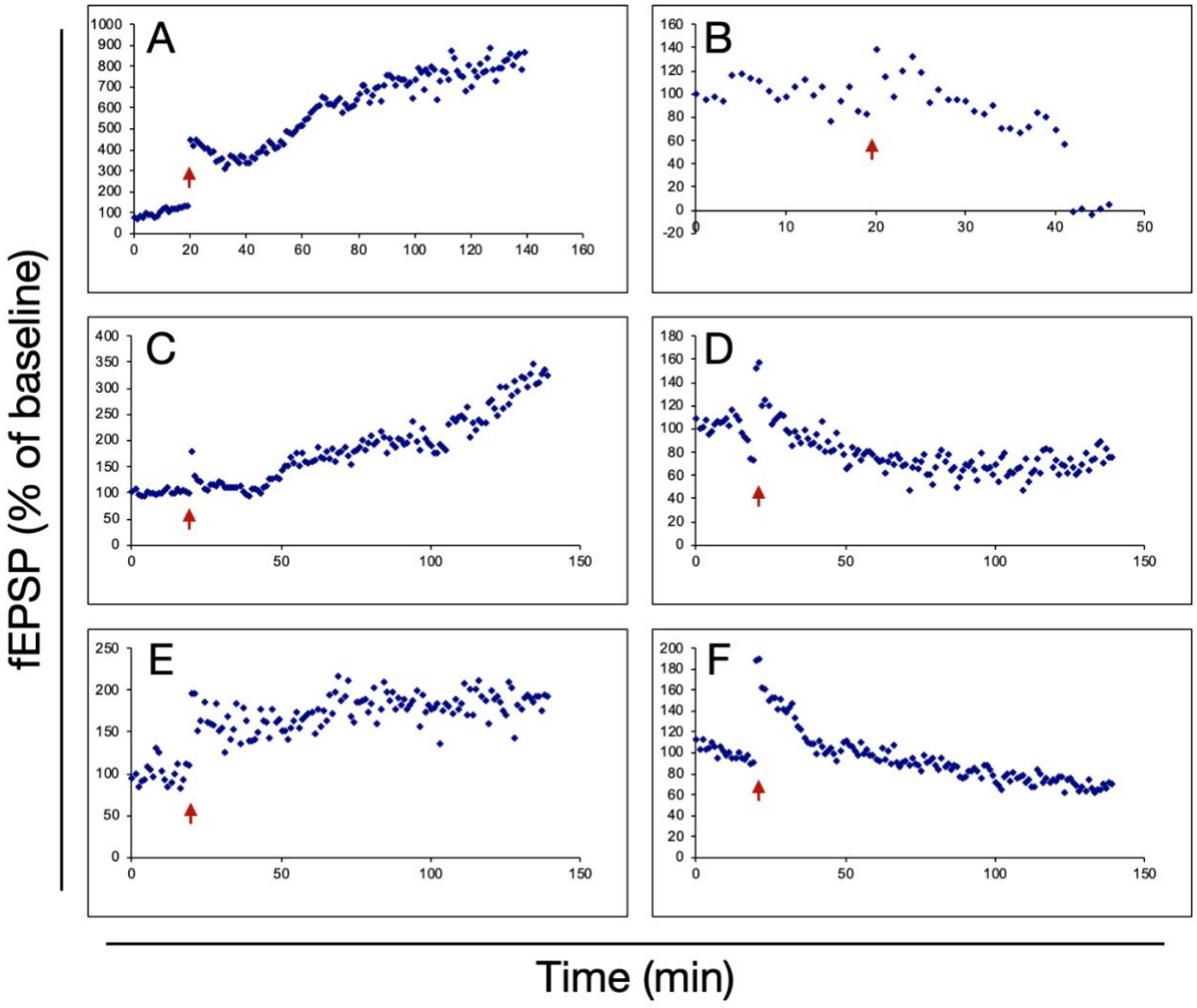

Figure 2.3.81: LTP induction attempts using the Axon Instruments rig. Red arrows indicate the time at which 1 x 100 Hz stimulation was applied. Y-axes represent the % change of fEPSP slope from baseline and X-axes represent time in minutes. A, C, & E) Depict examples where continuous increase in slope over time occurred (run-up). B, D, & F) Depict examples where there was continuous decrease in slope over time (run-down). Experiment B ended early at time ~45 minutes because of depleted DS3 Isolated Current Stimulator batteries. A different mouse was used for each graph.

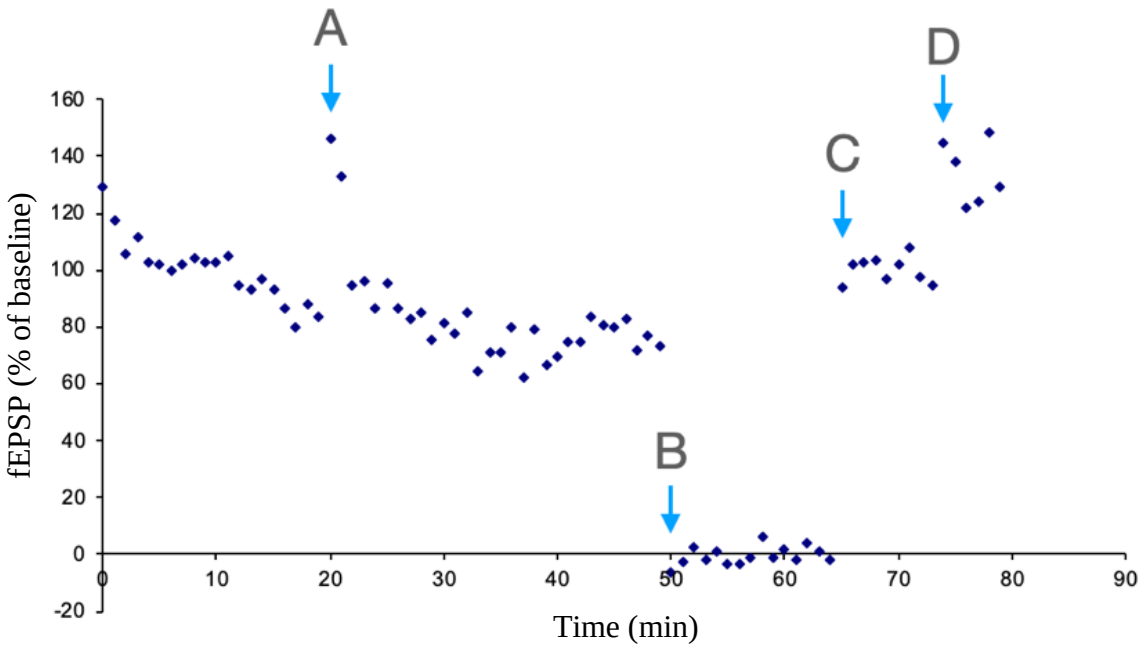

Figure 2.3.82: The effect of stimulator battery depletion on fEPSP slope. All data points are from the same slice and recording location. A) Application of 1 train LTP induction (1 x 100 Hz) at time 20 minutes. B) The sudden drop of slope to zero at time 50 minutes. C) The stimulator batteries were changed at time 65 minutes. D) LTP induction (1 x 100 Hz) was applied for a second time at 74 minutes. The stimulator used in this experiment was a Digitimer DS3 Isolated Current Stimulator requiring eleven 9V batteries.

2.4. DISCUSSION

2.4.1 Mouse hippocampal slice recording from the KSI rig

Recording from mouse hippocampal slices did not yield any waveforms that could be considered real fEPSPs. Despite extensive troubleshooting within the KSI Tissue Recording System, the reason behind why fEPSP waveforms were not observed is still unclear. This outcome could be due to several issues. Firstly, mechanical damage could be compromising slice health, resulting in the atypical field responses (Figure 2.3.32). If the damage occurred during the dissection process, it may be possible to improve this by dissecting under a microscope. For improved hippocampal slice preparation, Villers and Ris (2013) recommend dissecting under a surgical microscope (25X), and taking care to not touch or stretch the hippocampus, apart from gently

separating it from the cortex. Slice health issues could also be arising from the ingredients in the recovery and recording solution. Upon closer inspection, it was found that the $CaCl_2$ and $MgCl_2$ amounts listed were meant for 2M stock solutions; however, in the lab, the stocks were 1M. Thus, there was likely not enough $CaCl_2$ and $MgCl_2$ in the solutions. Low magnesium solutions have been found to evoke spontaneous seizure-like activity in hippocampal slices (Anderson *et al*., 1986; Walther *et al*., 1986). Additionally, a study by Rausche *et al*. (1990) found that lowered calcium concentration led to reduced CA1 responses and epileptiform activity. Thus, low concentration of magnesium and calcium in the surrounding solution may have caused irregular waveforms. Lastly, hippocampal slice responses may not have been visible due to high amounts of noise overpowering the signal. As demonstrated in Figure 2.3.42, the lowest amount of noise achieved was in the range of 10-14 mV; however, hippocampal fEPSP signals are typically below 5 mV. Thus, to improve hippocampal slice recording in the future, extra care should be taken to (1) further eliminate sources of background noise, (2) ensure solution ingredients are present in optimal concentrations, and (3) avoid mechanical damage.

2.4.2 Cricket cercal system activity

Recording from the cricket cercal system was explored as an alternative to using mice. Similar to findings in mouse hippocampal slices, no waveforms obtained resembled real fEPSPs (Figure 2.3.32). Reasons for this may include excessive background noise, suboptimal saline composition, and mechanical damage during dissection.

Another possibility is low health quality of the crickets used. Crickets were maintained on apple slices for 1-2 weeks, which is sufficient for short-term survival, but does not provide all nutrients required for sustained health. Clifford and Woodring (1990) recommend that, for

rearing and growth, crickets should be fed plant and animal sources of protein, which can be obtained from pre-made cricket food, such as Purina® Cricket Chow®. Another concern regarding the care of the crickets is that housing may have been overcrowded contributing to injury among crickets. Although no fighting was observed, there was one case where a cricket went missing, and only its leg was found later in the enclosure – evidence suggesting the cricket was cannibalized. Crickets do not normally eat each other unless they are starved or deprived of water (Clifford & Woodring, 1990); however the lack of protein in the diet may have contributed to this suspected behaviour.

2.4.3 Factors affecting background noise and stimulus artefact using the KSI rig

Reducing background noise is essential for measuring low amplitude biological signals, such as fEPSPs. Although improvements were made, further noise reduction would be ideal. For the KSI Tissue Recording System, the recommended acceptable level of interference is on the order of 25 μV peak to peak for 60 Hz noise (Kerr, 2009), which represents a major reduction from the 10-14 mV range currently present in the system. Further reduction of noise may be possible by securing the Faraday cage more tightly around the perimeter of the workspace, and devoting more time to proper grounding of equipment. One aspect of the workspace that has yet to be accounted for is the presence of grounding loops, where two elements thought to be grounded are connected to each other forming a circuit. Thus, there are additional factors to address in the future with regard to noise reduction.

Results of the present study demonstrated that solution concentration and volume affect background noise and stimulus artefact. There are a number of theories for why this might be. Firstly, at low NaCl concentration, there may have been less substrate for a reaction to take place

at the electrode, resulting in broken intervals of electron release, rather than a continuous uniform electron stream. Secondly, there may have been more noise at high volume because the electrodes were immersed in more solution, resulting in greater surface area for chemical reactions to take place. This could have potentially amplified the noise signal. Consistent with this theory is the observation that at high concentration and high volume, noise did not appear to increase (Figure 2.3.44 A, B), because amplification of a low noise signal should create a larger low noise signal. In contrast, amplification of a high noise signal should magnify that noise, which was observed in Figure 2.3.44 C, D. Lastly, stimulus artefact strength increased with higher solution concentration and lowered volume. This may have occurred because in higher concentration there are more charged particles for a stimulus to act on, resulting in a larger voltage change. Additionally, with high volume, the current injected by the stimulus may have more space to dissipate, resulting in a lower stimulus artefact signal. Interestingly, a previous study by Stecker *et al*. (2017) found an opposite effect of NaCl concentration on stimulus artefact, where increasing NaCl concentration reduced the artefact amplitude. This discrepancy may be attributed to the overall lower NaCl concentration used in the study, as well as the lower strength of current injection. Perhaps the effect of NaCl on stimulus artefact differs depending on the range of concentration and current injection used. Taken together, the results of Stecker *et al*. (2017) and the present study support the idea that stimulus artefact can potentially provide important insights into the properties of the surrounding solution.

2.4.4 fEPSP run-up and run-down

fEPSPs were able to be recorded when using the Axon Instruments rig, and all components of the waveform were visible, including the presynaptic fibre volley (Figure 2.3.7B). LTP was successfully induced, with the slope of the fEPSP increasing noticeably after 1 x 100Hz high

frequency stimulation (Figure 2.3.81). However, the LTP attempts showed signs of run-up and run-down. Run-up refers to a steady increase in slope over time, while run-down refers to a steady decrease in slope. This can be an indication that the slices are not healthy or that there is something wrong with the electrodes. Abrahamson *et al*. (2016) suggest a number of reasons for why this might occur in slice recordings. It may be the case that the electrodes are drifting (gradually moving); the slice may be subtly shifting position; the oxygen levels may be dropping or increasing; temperature could be changing; and/or the slice may be damaged (Abrahamson *et al*., 2016). Furthermore, it appears that declining battery life in the amplifier also results in run-down (Figure 2.3.82). In order to improve the LTP response and eliminate run-up and run-down, all these factors must be considered.

CHAPTER 3: CHARACTERIZING SNAPTIC PLASTICITY IN THE PGE2 MOUSE MODEL OF AUTISM

3.1 INTRODUCTION

3.1.1 PGE_2 mouse model of autism

Lipids have structural and functional roles in the brain. They form the cell membrane of neurons and are involved in signal transduction (Agranoff *et al*., 2005). Prostaglandin E_2 (PGE_2) is a lipid molecule that has hormone-like effects in the brain and throughout the body. For example, it induces smooth muscle contraction, influences blood pressure, regulates body temperature, and is involved in inflammation processes (Legler *et al.*, 2010). PGE_2 is formed from membrane phospholipids. The tail of the phospholipid consists of the fatty acid arachidonic acid (AA). AA is separated from the phospholipid head by the enzyme phospholipase A_2, and is then converted to prostaglandin by the enzyme cyclooxygenase (COX) (Legler *et al.*, 2010). Abnormal levels of prostaglandins during pregnancy have been associated with neurodevelopmental defects in the child, as evident from use of the drug misoprostol, a prostaglandin E_1 analog. Misoprostol is distributed under the brand name Cytotec®, and is used for prevention of gastric ulcers, labor induction, and abortion. The long-term developmental effects of *in utero* misoprostol exposure can be observed in abortion survivors, and has been shown to result in birth defects, such as clubfoot, cranial nerve abnormalities, and joint contractures. These defects may be caused by disruption of blood flow to the fetus during misoprostol-induced uterine contractions (Gonzalez *et al*., 1998). Möbius syndrome is a common outcome in abortion attempts using Cytotec (Pastuszak *et al*., 1998). Möbius syndrome is characterized by complete or partial nerve paralysis of the face, often accompanied by limb malformations and, less commonly, ocular nerve palsies and incomplete development of the tongue (Kumar, 1990). Autism often co-occurs with Möbius

syndrome; a study by Strömland *et al.* (2002) examined 25 cases of Möbius syndrome and found 7 had autistic traits. This demonstrated that the likelihood of autism among people with Möbius syndrome is higher than among the general population. Furthermore, a study by Bandim *et al.* (2003) found, when examining the history of patients with a combination of Möbius syndrome and autism, there was an association between autism and fetal misoprostol exposure. Specifically, 3/5 of these children (60%) were positive for misoprostol exposure. Although misoprostol exposure during fetal development can be detrimental, exposure during birth, such as when used for labor induction, is not considered harmful for neurodevelopment. A study by Koenig *et al.* (2012) found no negative effects in mice injected with misoprostol, at clinical-level doses, and at post-natal day (pnd) 7, which correlates with human age at birth. In addition to learning about misoprostol exposure at birth, mice can be used to conveniently study misoprostol exposure during pregnancy and the subsequent neurodevelopmental effects on offspring. The PGE_2 mouse model of autism involves subcutaneous injection of PGE_2 into a pregnant mouse to mimic the effects of misoprostol. A study by Tamiji & Crawford (2010) found that misoprostol and PGE_2 act similarly on neuronal cells in culture by reducing the amount and length of neurite extensions. This provides evidence that, although misoprostol is a PGE_1 analog, it can likely exert similar effects in the brain as PGE_2. However, PGE_2 and PGE_1 have slightly different effects on uterine contractions, which is important to note because contractions may be responsible for disrupting blood flow to the fetus leading to birth defects (Marques-Dias *et al*., 2003). A study by Chiossi *et al*. (2012) found that PGE_1 produced significantly higher contractility in human myometrial (uterine) living tissue samples than PGE_2 during the first 180 minutes of exposure. Given the differences in action between PGE_2 and PGE_1 on uterine contractions, neurodevelopmental findings based on PGE_2 exposure during pregnancy may not

generalize to the effects of misoprostol exposure. However, the PGE_2 mouse model appears to display some autistic behavioural traits, which may be potentially useful for studying autism. Offspring of PGE_2-injected mice display abnormal social behaviour, as assessed by preference for objects over other mice in the 3-chamber test; repetitive behaviour, as assessed by increased propensity to bury marbles; and anxiety, as assessed by preference to stay along the edges of an open arena rather than the center (open field test) (Crawford, 2021). PGE_2 exposure may also affect forms of synaptic plasticity, such as long-term potentiation (LTP). Akaneya and Tsumoto (2006) found that PGE_2 enhances LTP in the rat visual cortex. They propose that this enhancement is due to trafficking of PGE_2 receptors, where theta burst stimulation helps produce PGE_2 at the postsynaptic membrane, leading to a shift in PGE_2 receptor composition. PGE_2 then binds to the receptors leading to the activation of CREB and synthesis of proteins needed for sustained L-LTP (Akaneya, 2007). Another study by Chen *et al*. (2002) found that PGE_2 is needed for normal LTP responses from the hippocampal perforant pathway. They found that LTP was reduced when slices were incubated in COX-2 inhibitors, but this reduction could be restored by exogenous application of PGE_2. This suggests that COX-2 regulates PGE_2, which is needed for proper LTP responses. Since synaptic plasticity is dependent on PGE2 signalling, perhaps its disruption during development will lead to noticeable LTP deficits in later life. This section explores if *in utero* exposure to PGE_2 leads to hippocampal synaptic plasticity changes in adult life.

3.1.2 Developmental differences of the mouse and human brain

The mouse brain develops and ages at an accelerated pace compared to humans. In general, roughly 9 days of a mouse's life is equivalent to 1 human year, but this varies depending on life stage. For example, during the weaning period, mice develop slower compared to development

during the juvenile stages (Dutta & Sengupta, 2016). In terms of brain development, a review by Semple *et al*. (2014) highlights the ages at which mice and humans share important milestones. They note that axon and dendrite density increases during the mouse pnd 7-10, similar to the human brain of a newborn infant; the prefrontal cortex structurally matures at pnd 20-21, similar to a 4-10 year old human child; and the brain takes on distinct adult characteristics (synaptic density, neurotransmitter, myelination, and grey matter levels) at pnd 60+, similar to a 20+ year old human. Although the function of the hippocampus in memory is conserved across mammalian species (Allen & Fortin, 2013), its structural morphology is simplified in mice compared to humans. In rodents, the excitatory connections in the CA1 region are more clearly delineated to specific layers, whereas, in humans, the apical and basal dendrites overlap and do not separate into specific layers, suggesting connectivity differences between species (Benavides-Piccione *et al*., 2020). In support of connectivity differences, Bergmann *et al*. (2016) observed with fMRI that the mouse hippocampus is functionally connected to cortical sensory networks, while the human hippocampus is functionally connected to cortical association areas. This implies that sensory information is relayed to association areas before connecting with the hippocampus in humans, whereas in mice, sensory processing from the cortex channels directly to the hippocampus. The hippocampus varies in size and shape across different mammals, such as rodents, rabbits, monkeys, and humans, but it retains a set of distinct morphological areas, including the CA regions and dentate gyrus (Andersen *et al*., 2006). Differences and similarities have been observed in the development of the hippocampus between mice and humans. A study by Zhong *et al*. (2020) found that gene expression in the hippocampus of humans at gestational week 16-27 was most similar to hippocampal gene expression in mice at pnd 0-5; however, the overall correlation between mice and human gene expression during these time periods was

approximately 0.5 or less. The mouse brain has its differences from the human brain in terms of development and structure; however, when research requires the use of mice, particularly in the study of the hippocampus, the similarities prove useful. Studies on mice can lead to important insights about humans, as long as we remember to take into account the differential developmental timelines, morphology, and functional connections.

3.2 MATERIALS AND METHODS

3.2.1 Generating the PGE_2-injected mouse model of autism

All mice were housed at the York University animal facility, department of Biology (Toronto, ONT, Canada), maintained on a 12hr light/dark cycle with food and water available *ad libitum*. Protocols were approved by the York University ACC. C57BL/6 pregnant mice were injected with PGE_2 at embryonic day 11 (E11). The subcutaneous injection was applied dorsally between the skin and muscle at the base of the neck. 0.25µg of 16, 16-dimethyl prostaglandin E2 (item number 14750; Cayman Chemical Company) was injected per gram of mouse. The injection volume was fixed at 300uL with mixture of saline. Pregnant control mice were injected using the same procedure, except using saline only rather than a saline-PGE_2 mixture. Offspring of the injected pregnant mice became the experimental subjects at postnatal day 92-120 (P92-P120). All experiments were conducted using the Axon Instruments electrophysiology rig (see section 2.2.3 for details about slice recording using this system). For dissection and slicing procedures see chapter 2 methods page 24.

3.3 RESULTS

3.3.1 Defining electrophysiological properties in the hippocampus of the PGE2-injected mouse model of autism

With the Axon Instruments rig set up for electrophysiological recordings, I could next investigate fEPSP properties in the hippocampus of specific autism mouse models. A readily available autism model was the PGE_2-injected mouse, generated and provided by PhD student Ashby Kissoondoyal from Dr. Dorota Anna Crawford's lab at York University. All experiments were conducted on male mice age 13-17 weeks (P92-P120). The control group (saline-injected) consisted of 3 mice (n=3) from the same litter. The experimental group (PGE_2-injected) consisted of 4 mice (n=4), 3 from the same litter and 1 from a different litter. Sample sizes were the same for all experiments: input-output curves, E-LTP, and paired-pulse facilitation. Each experiment was run on a different hippocampal slice. For example, 3 slices were used per mouse; one for the input-output responses (Figure 2.3.1), one for long-term potentiation (Figure 2.3.2), and one for paired-pulse facilitation (Figure 2.3.3).

3.3.2 Input-output responses

To investigate differences in basal synaptic response, input-output curves were produced (Figure 3.3.2D). Input-output curves are generated by measuring the slope of the fEPSP (Figure 3.3.2E) in response to increasing stimulus intensity. It was found that the PGE_2-injected group had significantly lower synaptic response to increasing stimulus intensity (Figure 3.3.2A), as assessed by two-way ANOVA. However, the variation between the two groups differed significantly (Figure 3.3.2B). To ensure the number of axons activated was consistent between the two groups, the presynaptic fiber volley amplitudes were plotted and found to not differ significantly (Figure 3.3.2C).

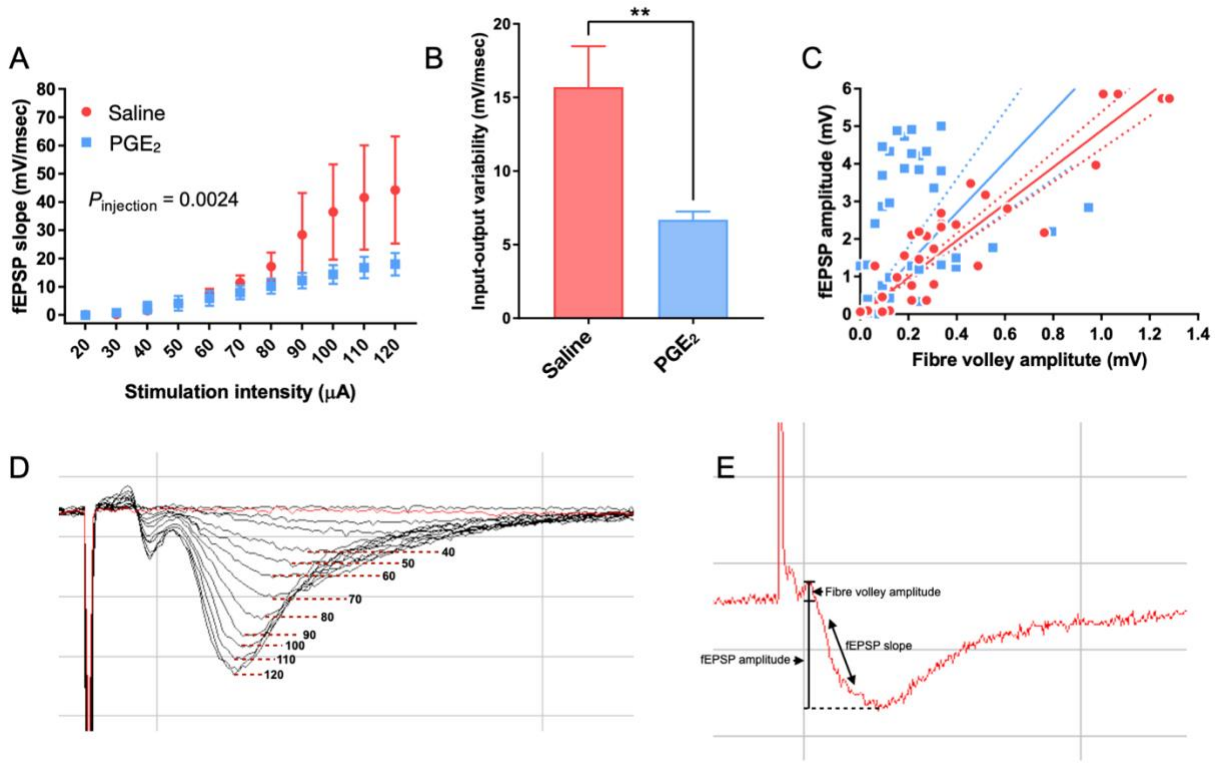

Figure 3.3.2: Control input-output responses were stronger and more variable than the PGE$_2$-injected group. A) There was an overall significant difference in input-output response between injection groups (P = 0.0024, determined by two-way ANOVA). Data represent means ± SEM. B) Input-output variability was higher in the saline group, P = 0.001 as determined by Levene's test (one-way ANOVA on the difference between the slope values and their group mean). Data represent means of variability (average difference between the slope values and their group mean) ± SEM. C) Plot of all input-output values as a function of fibre volley amplitude and fEPSP amplitude. Solid lines represent lines of best fit; slope values ± SEM are 4.889 ± 0.2406 for the saline group and 6.742 ± 1.117 for the PGE$_2$ group. Dotted lines indicate 95% confidence intervals. D) An example of an input-output curve. Input-output responses were measured by increasing stimulus intensity by 10μA increments each minute and recording the waveform response. Numbers and dotted lines represent the μA value that elicited the corresponding waveform. E) An example of how parameters are measured from a hippocampal field response, including presynaptic fibre volley amplitude, fEPSP amplitude, and fEPSP slope.

3.3.3 Early long-term potentiation

To determine if LTP was affected by prenatal PGE$_2$-injection, single-train (early) LTP was induced. Outcomes of individual trials are shown in Figure 3.3.31, where A, C, and E represent the control slices, while B, D, and F represent the experimental slices. The control trials appeared to have some abnormalities, such as run-up (Figure 3.3.31A), visibly high variation (Figure

3.3.31C), and run-down (Figure 3.3.31E). In contrast, the experimental trials did not demonstrate run-down, or run-up. Combining all trials into an average of their respective groups (Figure 3.3.32A) revealed excessive variation in the control group (Figure 3.3.32C). Overall, there appeared to be no significant differences in LTP between the two groups; however, when examining only the first 10 minutes (Figure 3.3.32B), the PGE_2-injected group had significantly higher potentiation than the control, as assessed by two-way ANOVA.

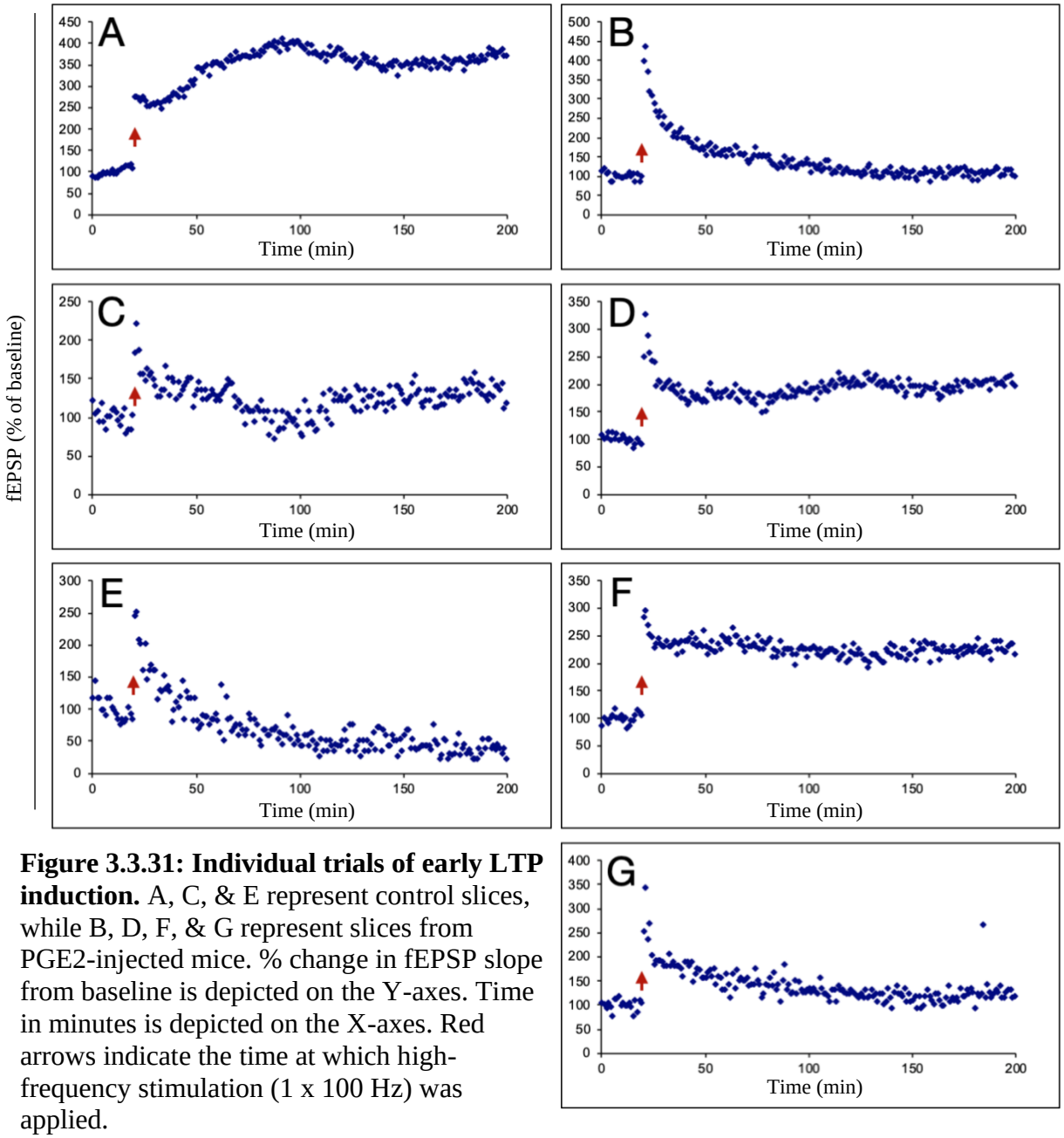

Figure 3.3.31: Individual trials of early LTP induction. A, C, & E represent control slices, while B, D, F, & G represent slices from PGE2-injected mice. % change in fEPSP slope from baseline is depicted on the Y-axes. Time in minutes is depicted on the X-axes. Red arrows indicate the time at which high-frequency stimulation (1 x 100 Hz) was applied.

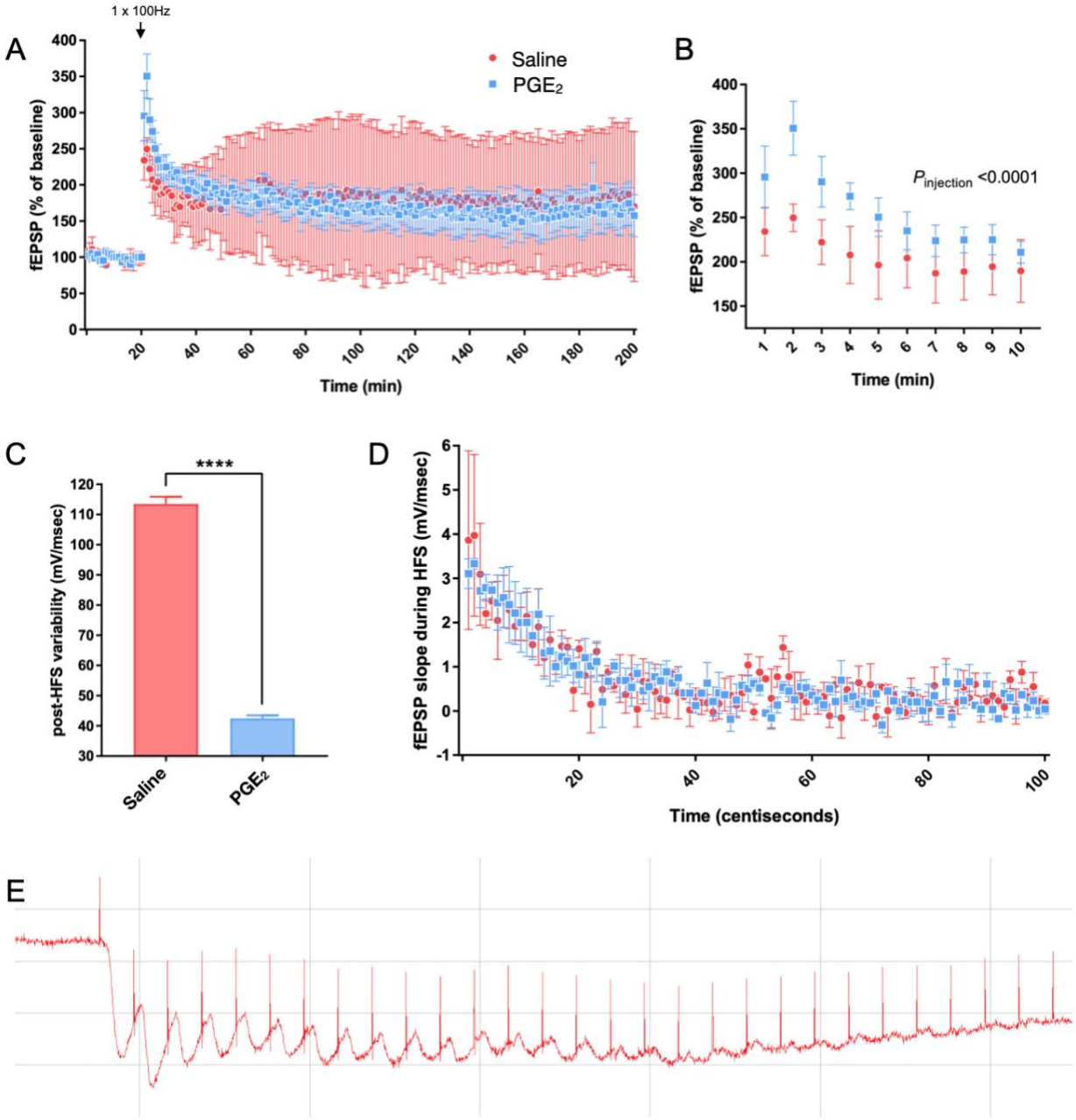

Figure 3.3.32: The saline-injected group had reduced potentiation and higher variability following high-frequency stimulation (HFS). A) There were no significant differences in long-term potentiation (LTP), as determined by two-way ANOVA. Data represent means ± SEM. LTP is expressed as percentage of fEPSP slope change compared to the average baseline slope. The black arrow denotes the time point at which HFS (1x100 Hz) was applied. The slice was stimulated once per minute for 3 hours and 20 minutes total; the first 20 minutes were baseline fEPSP recordings, then HSF (rapid succession of 100 stimuli in 1 second) was applied, after which fEPSP recordings continued once per minute for 3 hours. B) A closer analysis of the first 10 minutes following HSF revealed a significant difference between injection groups ($P <$ 0.0001, as determined by two-way ANOVA). C) LTP variability was higher in the saline group, $P < 0.0001$ as determined by Levene's test. Data represent means of variability (average

difference between the slope values and their group mean) ± SEM. D) There were no significant differences in fEPSP slopes generated during HFS. E) An example of fEPSP recordings during HFS.

3.3.4 Paired-pulse facilitation

To determine if differences in short-term presynaptic plasticity exist in PGE_2-injected mice, I conducted paired-pulse facilitation (PPF), which is measured as the slope of the second fEPSP in short succession divided by the slope of the first fEPSP (Figure 3.3.4B). There were no significant differences found with regard to PPF between the two groups (Figure 3.3.4A).

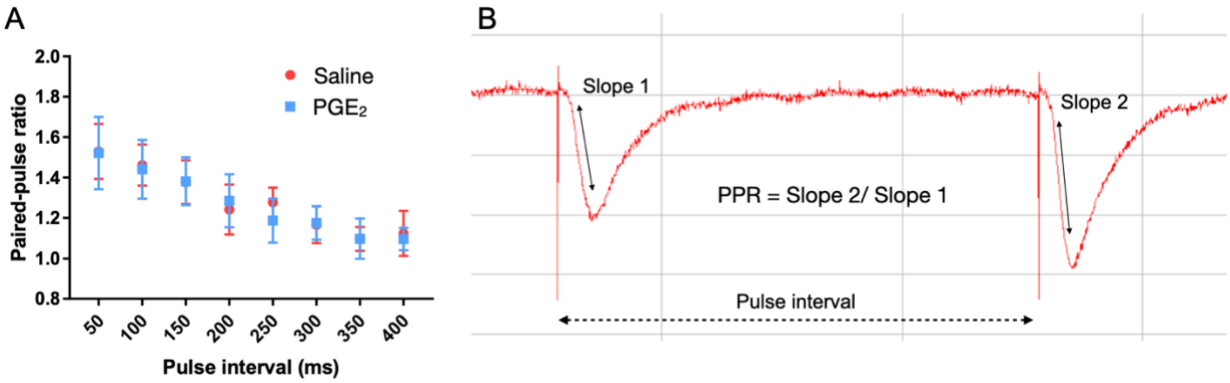

Figure 3.3.4: Short-term presynaptic plasticity was similar for both injection groups as measured by paired-pulse facilitation (PPF). A) There were no significant PPF differences, as assessed by two-way ANOVA. B) A diagram showing how paired-pulse ratio (PPR) is determined. For each pulse interval, 4 recordings were taken and an average of the 4 PPRs was used as the final value for that slice (n=3 slices for the control saline group and n=4 slices for the PGE_2 group).

3.4 DISCUSSION

3.4.1 Synaptic plasticity differences between saline- and PGE_2-injected mice

The PGE_2-injected mice appear to have similar E-LTP (Figure 3.3.32) and paired-pulse facilitation (Figure 3.3.4) as compared to the saline-injected mice. However, there were some notable differences; basal synaptic response was lower, and potentiation during the first 10 minutes after HFS was enhanced in the PGE_2-injected group (Figure 3.3.2; Figure 3.3.32B). This

may indicate a higher responsiveness to HFS in the PGE_2 group, perhaps due to developmental and structural changes caused by *in utero* PGE_2 exposure. Since exogenously applied PGE_2 is known to enhance potentiation in hippocampal slices (Chen *et al*., 2002) through a mechanism thought to involve PGE_2 receptor upregulation (Akaneya, 2007), it may be possible that early exposure to PGE_2 influences PGE_2 receptor composition. It could also be possible that the lowered basal synaptic response allows for a greater % change in potentiation following HFS. However, the effect of heighted potentiation may be the result of other confounding factors related to the experimental procedure. Based on the individual trials of LTP induction (Figure 3.3.31), there is a possibility that the slices of the control group were not as healthy as the slices in the experimental group, which could account for the diminished potentiation response of the control. All three trials of the control group had visible abnormalities, including run-up (Figure 3.3.31A), run-down (Figure 3.3.31E), and heightened variability (Figure 3.3.31C). Some of these issues could be observed in the experimental group, but to a much lesser extent. For example, there was slight run-up in trial D and slight run-down in trial B. Given that run-up and run-down could indicate poor slice health, drifting electrodes, gradual shifts in position of the slices, temperature changes, and/or oxygen level changes during the experiment (Abrahamsson *et al*., 2016), there is concern that the findings of higher potentiation in the experimental group could simply be due to these procedural factors. On the other hand, it could be the case that the PGE_2 model's hippocampus is less susceptible to run-up and run-down, and the procedural factors that often cause these effects. Perhaps PGE_2-induced alterations afford the hippocampus a higher level of robustness and ability to stay 'healthy' despite inevitably harmful experimental conditions (i.e. slicing and maintenance in an artificial setting).

When trying to identify the mechanism of action that *in utero* exposure to PGE_2 has on development, it can be difficult to discern whether effects are due to direct PGE_2 exposure or indirect ischemia. In humans, Möbius syndrome is thought to be caused by abortion attempts using misoprostol because the resulting uterine contractions restrict blood flow to the fetus, damaging the facial nerves (Gonzalez *et al*., 1998). Thus, when studying the physiological differences of PGE_2 mice, one can question whether the differences are connected to early restriction of blood flow, and/or direct exposure to heightened PGE_2 levels in the body.

More studies will be needed to determine if LTP and other forms of synaptic plasticity are altered in the PGE_2 mouse model of autism. The present study is limited by small sample size, run-up and run-down on control trials, and exclusion of female mice.

CHAPTER 4: THERAPEUTIC APPLICATIONS AND UTILITY OF ASD MOUSE MODELS

4.1 INTRODUCTION

4.1.1 Hebbian and homeostatic plasticity in autism spectrum disorder

Connections between neurons, known as "synapses", can be strengthened with learning or weakened with forgetting – changes which represent the "Hebbian" form of plasticity (Cruikshank & Weinberger, 1996). Hebbian plasticity was first postulated by Donald Hebb in 1932 as a process whereby repeated firing between two neurons strengthens the connection between them (Brown & Milner, 2003). Hebb's postulate was later confirmed with experimental evidence when, in 1973, Bliss and Lømo reported long-term potentiation (LTP); they observed that when neurons are repeatedly induced to fire by electrical stimuli, a subsequent long-lasting state of heightened synaptic strength occurs. Their observations supported Hebb's postulate by demonstrating that when connected neurons fire often over time, the specific response between those neurons is enhanced. In contrast to the specificity of Hebbian plasticity, homeostatic plasticity acts by globally scaling neuronal activity to maintain balance and prevent over- or under-excitation (Turrigiano & Nelson, 2004). For example, it has been observed that chronically blocking neuron activity results in subsequent hyper-excitability once the blockade is removed, presumably due to the homeostatic mechanism working to maintain a set-point level of network activity (Ramakers *et al*., 1990; Van Den Pol *et al*., 1996). Maintenance of a target activity range is essential to ensure optimal functioning because Hebbian mechanisms can lead to increasing extremes of excitatory or inhibitory synaptic strength (Turrigiano & Nelson, 2004). Given that the interaction between Hebbian and homeostatic plasticity is essential for proper learning and

memory formation, it raises an interesting question of how these processes may be altered in ASD.

The aberrations in synaptic composition apparent in ASD may be due to lack of coordination between Hebbian and homeostatic forms of plasticity. For instance, it is well known that ASD is marked by imbalances of excitatory to inhibitory synapses (E/I ratio) (Nelson & Valakh, 2015), as demonstrated by reports of over-excitation in the brains of those with ASD (Takarae & Sweeney, 2017) and frequent co-occurrence with seizures (Tuchman & Rapin, 2002) (an outcome of hyper-excitation). Moreover, there is evidence to support that when excitatory synapses are saturated, it becomes more difficult to learn and encode new information (Kuhn *et al*., 2016). Thus, I hypothesize that homeostatic scaling, targeted toward alteration of global excitatory or inhibitory synaptic strength, can mitigate E/I ratio imbalances and restore Hebbian plasticity in an ASD mouse model.

4.2 METHODOLOGY PLANNING

4.2.1 Designing methods for testing homeostatic-Hebbian interaction

Before testing homeostatic-Hebbian interaction it is necessary to devise the methodology. The general idea for the procedure is to harvest hippocampal slices from the mouse brain (Fig 4.2.11), and then incubate the slices in drugs that can induce homeostatic scaling, such as the sodium channel blocker tetrodotoxin (TTX), and the NMDA receptor antagonist 2-amino-5-phosphonopentanoic acid (AP5). Following washout, LTP induction by high-frequency stimulation will be applied to the CA3-CA1 synaptic pathway within stratum radiatum to determine how homeostatic plasticity alters Hebbian plasticity (Fig 4.2.12).

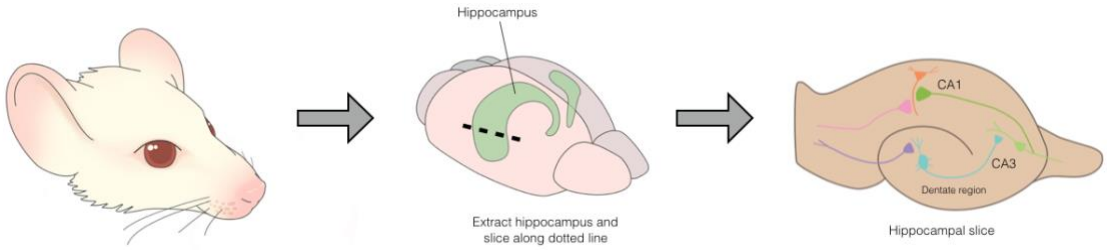

Figure 4.2.11: Hippocampal slice preparation from whole mouse brain.

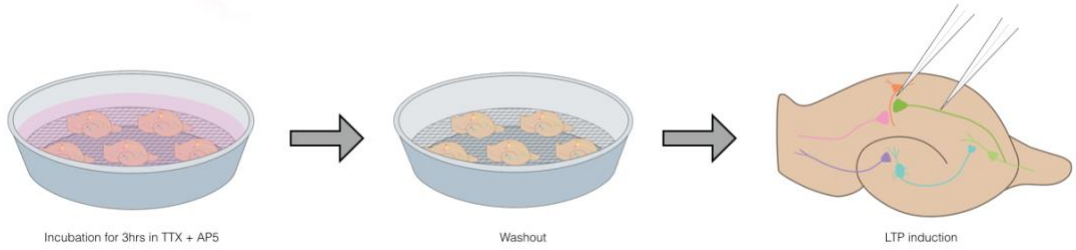

Figure 4.2.12: Procedure for studying homeostatic scaling and Hebbian LTP interaction.

Some of the main questions related to this experimental protocol are 1) how to apply the drug treatments for homeostatic scaling and 2) which autism mouse model(s) would be most appropriate for use?

4.2.2 Troubleshooting incubation chambers for drug application

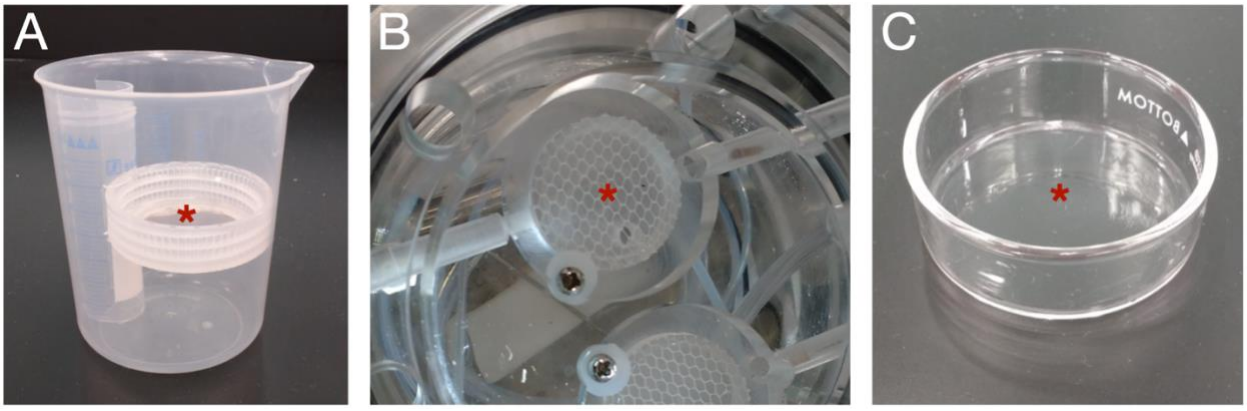

Figure 4.2.21: Options available for drug treatment incubation of hippocampal slices. The submersion chamber (A) holds slices 4-5 cm below the saline. The interface chamber (B) holds slices ~0.5 mm below the saline, and is used during the recording process as well. The glass Petri dish (C) holds the slices ~1 cm below the saline. Red asterisks denote the location of the slices during the incubation period.

Three methods for drug treatment incubation were tested, namely the submersion chamber, interface chamber, and glass Petri dish (Figure 4.2.21). When slices were incubated in the submersion chamber (Figure 4.2.21A) for 2.5 hours, no fEPSPs were able to be found after subsequent transfer to the interface chamber for recording. Some irregular waveforms were noted, which did not resemble the characteristic fEPSP shape, suggestive of mechanical damage to the slices. Since incubation in the submersion chamber did not appear ideal, I ran a test to see if slices could be incubated successfully in the interface chamber or simply in a glass Petri dish with oxygen supply. It was found that a 2.5 hour incubation in the interface chamber or the glass Petri dish yielded similar fEPSP responses and LTP (Figure 4.2.22).

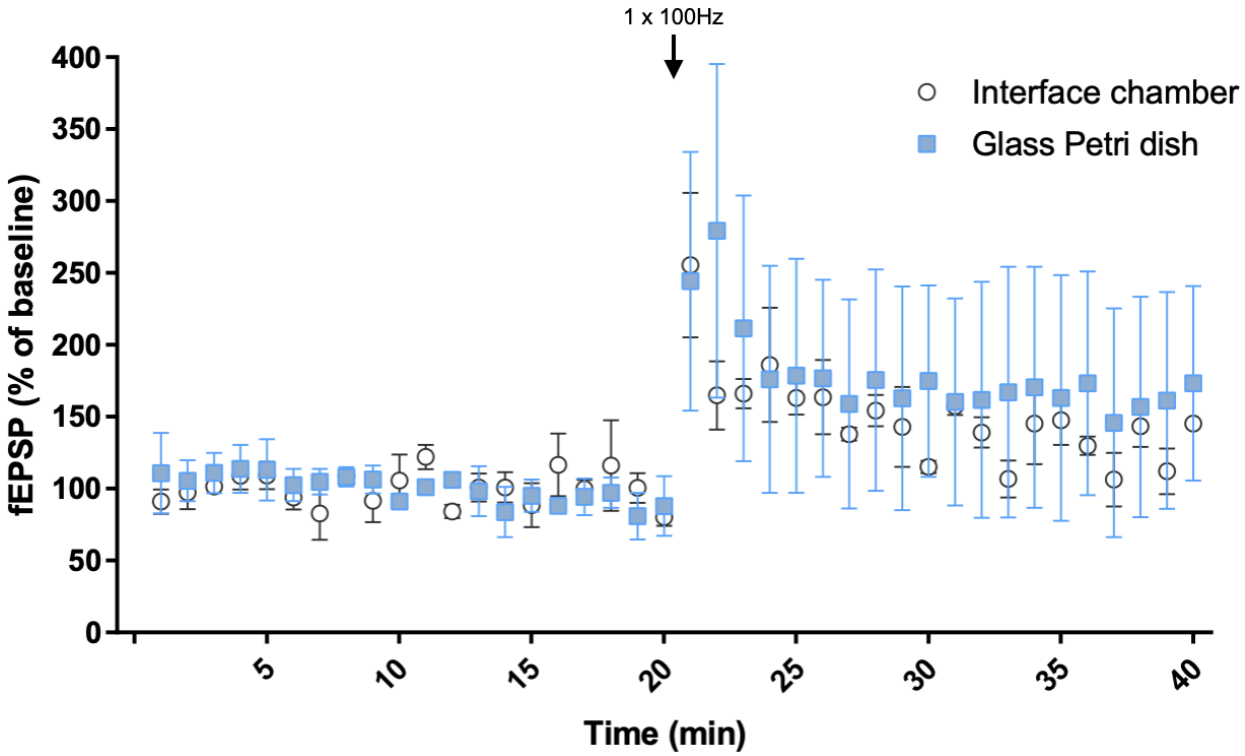

Figure 4.2.22: High frequency stimulation produces similar potentiation effects in slices incubated in a heated interface chamber and room temperature Petri dish. Slices were incubated for 2.5 hours in either an interface chamber heated to 30°C, or a glass Petri dish at room temperature. n=3 slices for the interface chamber group, and n=3 slices for the glass Petri dish group. All slices were obtained from one mouse, with left and right hippocampal slices randomized. There were no significant differences, as assessed by two-way ANOVA with Bonferroni's multiple comparisons test.

4.2.3 Determining autism mouse models suitable for testing homeostatic-Hebbian interaction

There are hundreds of mouse models that can be used to study autism, created with gene and/or environmental manipulations leading to autism-like phenotypes. Deciding which model to use depends upon which aspect of autism is of interest to the study. Since my study focused on the role of homeostatic plasticity in ASD, and the ability of excitatory downscaling to restore LTP, I was searching for a mouse model with impaired LTP and evidence of heightened excitability within the brain. My original plan was to work with *Mdga2*$^{+/-}$ mice, which fit these criteria; however, due to lack of availability, alternative mouse model(s) would be needed. I explored some common ASD models, including *Shank3B* knockout, *Shank1* knockout, *Fmr1* knockout, PGE2-injected model, neuroligin-3-deficient model, black and tan brachyury (BTBR) inbred strain, and *Pten* knockout (Table 4.2.31). I evaluated each of these models based on autism phenotype, impairment of LTP, availability, and E/I ratio (Table 4.2.32). The models with the highest score were deemed most appropriate for experimental study going forward, which proved to be the BTBR inbred strain and *Shank3B* knockout. Both of these models had a score of 18, but the distribution of points varied with the BTBR strain scoring higher on evidence for elevated E/I ratio and the *Shank3B* knockout scoring higher on evidence for impaired LTP.

Table 4.2.31: Collection of relevant information for comparing autism mouse models for use in the homeostatic-Hebbian interaction experiment.

Model	How to generate?	Autistic behavioural traits	Autistic physiological traits	LTP information	E/I ratio information	How to order?
PGE_2-injected	Injection of pregnant mouse with PGE_2 at E11. Offspring are used as the autism model, representing prenatal environmental exposure to PGE_2.	Repetitive behaviour (increased grooming and marble burying), social abnormalities (Crawford, 2021).	Differential expression of Wnt-regulated genes (Rai-Bhogal, 2018).	Some weak evidence of heightened LTP (see chapter 3)	N/A	Generate with PGE_2 injection of common C57BL/6 mice (Jackson Laboratory ~$30 per mouse).
***Shank3B*$^{-/-}$**	*Shank3*^{tm2Gfng}/J; Neo cassette replacing exons 13-16 of the *Shank3* gene on chromosome 15, altering expression of the *Shank3b* isoform (jax.org).	Self-injurious repetitive grooming, deficits in social interaction, anxiety-like behaviour (Peça *et al*., 2011). Deficits in vocalizations, learning, and memory (Dhamne *et al*., 2017).	More prone to having seizures, enlarged caudate volume (Peça *et al*., 2011). Altered dendritic spine morphology (Wang *et al*., 2011).	Reduced LTP and similar LTD in hetrozygotes (Bozdagi *et al*., 2010).	Homeostatic plasticity deficits in *Shank3* mRNA knock down in neuronal cell culture (assessed by upscaling using application of TTX) (Tatavarty *et al*., 2020). Reduced E/I ratio in hippocampus (Lee *et al*., 2015).	Jackson Laboratory ($255 per heterozygous mouse).

Model	How to generate?	Autistic behavioural traits	Autistic physiological traits	LTP information	E/I ratio information	How to order?
***Shank1*$^{+/-}$, *Shank1* $^{-/-}$**	Targeted null/knockout; *Shank1*^{tm1Shng}/J; replacement of exons 14 and 15 on chromosome 7 with a PGK-neomycin drug resistance cassette (jax.org).	Repetitive behaviour (increased grooming, but reduced marble burying) (Sungur *et al*., 2014), mild anxiety-like behaviour (Gong & Wang 2015). *Shank1*$^{-/-}$ demonstrate reduced exploratory locomotion, motor coordination, balance and neuromuscular strength (Gong & Wang, 2015). Social deficits evaluated by ultrasonic vocalizations (Gong & Wang, 2015). Impaired contextual fear memory (Hung *et al*., 2008). However, *Shank 1*-/- and -/+ do not prefer a novel object over a novel mouse, -/- prefer the novel mouse, indicating normal social behaviour (Silverman *et al*., 2011).	Altered denritic spine morphology (Hung *et al*., 2008; Martínez-Cerdeño, 2017).	Similar LTP and LTD (Hung *et al*., 2008).	*Shank1*$^{-/-}$ has increased E/I ratio in hippocampal CA1 pyramidal neurons (Mao *et al*., 2015).	Cryo recovery from Jackson Laboratory ($2854 USD per mouse, 12-week process).
Neuroligin-3-deficient (*Nlgn3*^{R451C})	*Nlgn3*$^{tm1.1Htz}$/J; CGT in exon 6 of chromosome X encoding arginine at amino acid position 451 was modified to cysteine (TCG).	Enhanced formation of repetitive motor routines (Rothwell *et al.*, 2014). Elevated aggression, repetitive behaviour (visitations to novel objects), impaired juvenile social interaction (Burrows *et al*., 2015).	Increased dendritic branching in the stratum radiatum of the CA1 region of the hippocampus (Etherton *et al*., 2011).	Increased LTP (Etherton *et al*., 2011).	Evidence for decreased E/I ratio due to enhanced GABAergic transmission in the somatosensory cortex and increased frequency of spontaneous IPSCs (Tabuchi *et al*., 2007).	Cryo recovery from Jackson Laboratory ($2854 USD per mouse, 12-week process).
***Mdga2*$^{+/-}$**	The coding sequence in first exon of *Mdga2* is replaced by a *LacZ-pA-PGK-Neo-pA* cassette.	Stereotypy, aberrant social interactions, impaired memory and hippocampal-dependent learning (Connor *et al*., 2016).	Increased synaptic density (Connor *et al*., 2016; Tang *et al*., 2014).	Enhanced E-LTP, impaired L-LTP (Connor *et al*., 2016).	Increased E/I ratio (increased excitatory synaptic density and transmission in the hippocampus) (Connor *et al*., 2016).	Potentially available from Dr. Tohru Yamamoto, Kagawa University, Japan.

Model	How to generate?	Autistic behavioural traits	Autistic physiological traits	LTP information	E/I ratio information	How to order?
***Fmr1* knockout**	Fmr1^{tm1Cgr}/J; neomycin resistance cassette replacing exon 5 of fragile X mental retardation syndrome 1 (*Fmr1*) gene (jax.org).	Atypical social interactions; deficits in learning, memory, and reversal learning; hyperactivity; altered response to sensory stimuli (Bernardet & Crusio, 2006).	Altered myelin expression in the corpus callosum (Lee *et al*., 2019). Increase in GFAP expression and astrocyte hypertrophy (Lee *et al*., 2019; Bronzuoli *et al*., 2018).	LTP reduced in the dentate gyrus, but intact in the CA1 (Bostrom *et al*., 2013). mGluR-LTD is augmented in the absence of FMRP (Huber *et al*., 2002).	Impaired homeostatic downscaling by treatment with picrotoxin (PTX) (Lee *et al*., 2018). Reduction of E/I ratio in layer 4 barrel cortex stellate cells (Domanski *et al*., 2019).	Jackson Laboratory ($236.78 USD per mouse).
BTBR *T*$^{+}$ *Itpr3*^{tf}/J	BTBR (Black and Tan BRachyury) inbred strain. Originally intended to be used to study insulin resistance and phenyloketo-nuria (Meyza & Blanchard, 2017).	Reduced social interactions, impaired play, low exploratory behavior, unusual vocalizations and high anxiety as compared to other inbred strains (Jax.org), increased self-grooming and marble burying (Amodeo *et al*., 2012).	Agenesis of corpus callosum (aCC) and reduction in the hippocampal commissure. Alterations in the morphology of the brain ventricles (Meyza & Blanchard 2017).	LTP (1 x 100Hz and 4x 100Hz) is similar in BTBR and C57BL/6, LTP slightly impaired with theta-burst stimulation, enhanced suseptibillity to depotentiation (MacPherson *et al*., 2008).	Evidence for elevated E/I ratio in hippocampal slices: reduced frequency of inhibitory post-synaptic current (IPSC) and increased amplitude/frequency of spontaneous excitatory post-synaptic current (EPSC) (Han *et al*., 2014).	Jackson Laboratory ($114.62 USD per mouse).
Pten neuron-specific knockout (NS-*Pten* KO)	GFAP-Cre; *Pten*$^{loxP/loxP}$ (Lugo *et al*., 2014).	Cerebellar Purkinje cell (PC) PTEN loss results in impaired sociability, repetitive behavior and deficits in motor learning. (Cupolillo *et al*., 2016). PTEN KO mice showed impaired performance on social behavioural tasks (social chamber and social partition test). They also showed increased repetitive behaviour (marble burying). No impact on ultrasonic vocalizations (Lugo *et al*., 2014).	PTEN mutations identified in 20% of children with ASD and macrocephaly and associated with white matter abnormalities (Busch, 2019). The Pten^{m3m4} model has altered gene expression related to myelination and increased thickness of the corpus callosum. (Frazier *et al*., 2015).	Contextual memory deficits (Lugo *et al*., 2013). Impaired synaptic plasticity (impaired CA3-CA1 response to 200 Hz tetanization) (Fraser *et al*., 2007). Deficits in LTP and LTD (Sperow *et al*., 2012).	Loss of *Pten* was found to increase both excitatory and inhibitory neuro-transmission in mouse hippocampal cell culture (Weston *et al*., 2014).	Generate with *Pten*^{flox} (Jackson Laboratory $255 USD per mouse) + cre recombinase neuron-specific strain (GFAP-cre).

Table 4.2.32: Scoring system applied to determine the most suitable autism mouse model(s) for use in exploring homeostatic-Hebbian interaction. Scores were assigned by a single rater on parameters of autism traits, impaired LTP, availability, and heightened E/I ratio. The top scoring models are highlighted in orange.

Model	Autism score (evaluation of autistic traits from 1-3; 1 point each for categories of communication, socialization, and repetitive behaviour)	LTP score (1 for normal LTP, 2 for evidence of impaired LTP)	Availability score (on a scale of 1-3 how easily can this model be ordered?)	E/I ratio score (1 for lowered, unknown, or normal E/I ratio, 2 for increased E/I ratio)	Total score (autism x LTP x availability x E/I ratio)
PGE2-injected	2	2	1	1	4
***Shank3B*$^{-/-}$**	3	2	3	1	18
***Shank1*$^{+/-}$, *Shank1* $^{-/-}$**	2	1	1	2	4
Neuroligin-3-deficient (*Nlgn3*^{R451C})	2	2	1	1	4
***Mdga2*$^{+/-}$**	2	2	1	2	8
***Fmr1* knockout**	1	2	3	1	6
BTBR *T*$^{+}$ *Itpr3*^{tf}/J	3	1	3	2	18
Pten neuron-specific knockout (NS-*Pten* KO)	2	2	2	1	8

4.3 DISCUSSION

Although Hebbian-homeostatic interaction in a mouse model of ASD has not been tested yet, the above methodology planning represents the first steps towards getting these experiments started. After troubleshooting the methods, it appears that an effective way to apply drug treatment is through the use of oxygenated solution in a glass Petrie dish at room temperature. Furthermore, although the *Mdga2*$^{+/-}$ mice are unavailable, the *Shank3B*$^{-/-}$ and/or BTBR *T*$^{+}$ *Itpr3*^{tf}/J mouse models of autism may serve as useful substitutes in these experiments.

The total score for the mouse models (Table 4.2.32) was obtained by multiplication rather than addition to help emphasize the divide between the options. Use of addition would give a similar outcome. The factors of autism score and availability score were weighted slightly higher (on a scale of 1-3, rather than 1-2) because these are essential attributes. For example, if the model is highly applicable to autism by demonstrating strong autism traits, then regardless of LTP or E/I ratio score, it may be worth using for exploration of homeostatic-Hebbian interaction. Availability was ranked similarly in weight as autism score because the experiments are heavily dependent on access to the mouse models. LTP and E/I ratio score were given slightly lower weights because regardless of how these appear individually, the experiment is assessing homeostatic-Hebbian *interaction*. Even though it would be ideal to explore a model with impaired LTP and heightened E/I ratio, models without this criteria will still be of interest for exploring homeostatic-Hebbian interface in autism.

In researching different types of autism mouse models, it is apparent that no one mouse model perfectly represents this disorder. Autism is complex, being caused by combinations of many different genes and environmental factors, and manifesting in symptoms that differ for each unique individual. Thus, when using mouse models to study autism, it is important to use a variety of types to best capture the wide spectrum of this disorder.

GENERAL CONCLUSION

The use of electrophysiology techniques to study synaptic plasticity in autism mouse models can reveal important functional insights, that would otherwise be impossible to study in humans. Optimization of equipment and planning of methodology are the first steps in tackling research questions related to this field. A large portion of this project focused on equipment set-up and troubleshooting (Chapter 2). Then in Chapter 3, synaptic plasticity was studied in the PGE_2 mouse model of autism, demonstrating reduced basal synaptic response and heightened potentiation during the first 10 minutes following HFS. Lastly, a potential therapeutic application of synaptic plasticity in autism was proposed, involving the interaction between Hebbian and homeostatic plasticity (Chapter 4). By understanding how synaptic plasticity is altered in ASD models and how it can be potentially restored, we are able to discover and support new avenues for ASD treatments and therapies.

REFERENCES

Abrahamsson, T., Lalanne, T., Watt, A. J., & Sjöström, P. J. (2016). Long-term potentiation by theta-burst stimulation using extracellular field potential recordings in acute hippocampal slices. *Cold Spring Harbor Protocols*, *2016*(6), pdb-prot091298.

Agranoff, B.W., Benjamins, J.A., & Hajra, A.K. (2005). Properties of Brain Lipids. *Basic Neurochemistry: Molecular, Cellular and Medical Aspects*, *33*.

Ahlsén, G., Rosengren, L., Belfrage, M., Palm, A., Haglid, K., Hamberger, A., & Gillberg, C. (1993). Glial fibrillary acidic protein in the cerebrospinal fluid of children with autism and other neuropsychiatric disorders. *Biological Psychiatry*, *33*(10), 734-743.

Akaneya, Y. (2007). The remarkable mechanism of prostaglandin E2 on synaptic plasticity. *Gene Regulation and Systems Biology*, *1*, 117762500700100009.

Akaneya, Y., & Tsumoto, T. (2006). Bidirectional trafficking of prostaglandin E2 receptors involved in long-term potentiation in visual cortex. *Journal of Neuroscience*, *26*(40), 10209-10221.

Al-Farsi, Y.M., Waly, M.I., Al-Sharbati, M.M., Al-Shafaee, M.A., Al-Farsi, O.A., Al-Khaduri, M.M., Gupta, I., Ouhtit, A., Al-Adawi, S., Al-Said, M.F. & Deth, R.C. (2013). Levels of heavy metals and essential minerals in hair samples of children with autism in Oman: a case–control study. *Biological Trace Element Research*, *151*(2), 181-186.

Allen, T. A., & Fortin, N. J. (2013). The evolution of episodic memory. *Proceedings of the National Academy of Sciences*, *110*(Supplement 2), 10379-10386.

Amodeo, D. A., Jones, J. H., Sweeney, J. A., & Ragozzino, M. E. (2012). Differences in BTBR T+ tf/J and C57BL/6J mice on probabilistic reversal learning and stereotyped behaviors. *Behavioural Brain Research*, *227*(1), 64-72.

Andersen, P., Morris, R., Amaral, D., Bliss, T., & O'Keefe, J. (Eds.). (2006). *The Hippocampus Book*. Oxford university press.

Anderson, W. W., Lewis, D. V., Swartzwelder, H. S., & Wilson, W. A. (1986). Magnesium-free medium activates seizure-like events in the rat hippocampal slice. *Brain Research*, *398*(1), 215-219.

Antoine, M. W., Langberg, T., Schnepel, P., & Feldman, D. E. (2019). Increased excitation-inhibition ratio stabilizes synapse and circuit excitability in four autism mouse models. *Neuron*, *101*(4), 648-661.

Asperger, H. (1944). Die “Autistischen Psychopathen” im Kindesalter. *European Archives of Psychiatry and Clinical Neuroscience*, *117*, 76-136.

Bailey, A. *et al*. (1998). Full genome screen for autism with evidence for linkage to a region on chromosome 7q. International Molecular Genetic Study of Autism Consortium. *Human Molecular Genetics,* 7, 571–578.

Bandim, J. M., Ventura, L. O., Miller, M. T., Almeida, H. C., & Costa, A. E. S. (2003). Autism and Möbius sequence: an exploratory study of children in northeastern Brazil. *Arquivos de Neuro-psiquiatria*, *61*(2A), 181-185.

Barrionuevo, G., Schottler, F. & G. Lynch. (1980). The effects of repetitive low frequency stimulation on control and "potentiated" synaptic responses in the hippocampus. *Life Sciences, 27*, 2385-2391.

Bear, M. F. (2005). Therapeutic implications of the mGluR theory of fragile X mental retardation. *Genes, Brain and Behavior*, *4*(6), 393-398.

Benavides-Piccione, R., Regalado-Reyes, M., Fernaud-Espinosa, I., Kastanauskaite, A., Tapia-González, S., León-Espinosa, G., Rojo, C., Insausti, R., Segev, I. & DeFelipe, J. (2020). Differential structure of hippocampal CA1 pyramidal neurons in the human and mouse. *Cerebral Cortex*, *30*(2), 730-752.

Bergmann, E., Zur, G., Bershadsky, G. & Kahn, I. (2016). The organization of mouse and human cortico-hippocampal networks estimated by intrinsic functional connectivity. *Cerebral Cortex*, 1-16.

Berlucchi, G. (2002). The origin of the term plasticity in the neurosciences: Ernesto Lugaro and chemical synaptic transmission. *Journal of the History of the Neurosciences 11*, 305-309.

Bernardet, M., & Crusio, W. E. (2006). Fmr1 KO mice as a possible model of autistic features. *The Scientific World Journal*, *6*, 1164-1176.

Bisazza, A. (1981). Social organization and territorial behaviour in three strains of mice. *Italian Journal of Zoology*, *48*(2), 157-167.

Bliss, T. & Lømo, T. (1973). Long-lasting potentiation of synaptic transmission in the dentate area of the anaesthetized rabbit following stimulation of the perforant path. *The Journal of Physiology*, *232*, 331-356.

Bliss, T. & Sam F. C. (2011). Long-term potentiation and long-term depression: a clinical perspective. *Clinics*, *66*, 3-17.

Bostrom, C. A., Majaess, N. M., Morch, K., White, E., Eadie, B. D., & Christie, B. R. (2015). Rescue of NMDAR-dependent synaptic plasticity in Fmr1 knock-out mice. *Cerebral Cortex*, *25*(1), 271-279.

Bozdagi, O., Sakurai, T., Papapetrou, D., Wang, X., Dickstein, D.L., Takahashi, N., Kajiwara, Y., Yang, M., Katz, A.M., Scattoni, M.L. & Harris, M.J. (2010). Haploinsufficiency of the

autism-associated Shank3 gene leads to deficits in synaptic function, social interaction, and social communication. *Molecular Autism*, *1*(1), 1-15.

Bronzuoli, M.R., Facchinetti, R., Ingrassia, D., Sarvadio, M., Schiavi, S., Steardo, L., Verkhratsky, A., Trezza, V. & Scuderi, C. (2018). Neuroglia in the autistic brain: evidence from a preclinical model. *Molecular Autism*, *9*(1), 1-17.

Brown, R. E., & Milner, P. M. (2003). The legacy of Donald O. Hebb: more than the Hebb synapse. *Nature Reviews Neuroscience*, *4*(12), 1013.

Bryant, C. D. (2011). The blessings and curses of C57BL/6 substrains in mouse genetic studies. *Annals of the New York Academy of Sciences*, *1245*, 31.

Bryda, E. C. (2013). The Mighty Mouse: the impact of rodents on advances in biomedical research. *Missouri Medicine*, *110*(3), 207.

Bucan, M., Abrahams, B.S., Wang, K., Glessner, J.T., Herman, E.I., Sonnenblick, L.I., Retuerto, A.I.A., Imielinski, M., Hadley, D., Bradfield, J.P. & Kim, C. (2009). Genome-wide analyses of exonic copy number variants in a family-based study point to novel autism susceptibility genes. *PLoS Genetics*, *5*(6), p.e1000536.

Bunyavanich, S., Donovan, M., Sherry, J., & Diamond, D. (2013). Immunotherapy for mouse bite anaphylaxis and allergy. *Annals of allergy, asthma & immunology: official publication of the American College of Allergy, Asthma, & Immunology*, *111*(3), 223.

Burrows, E. L., Laskaris, L., Koyama, L., Churilov, L., Bornstein, J. C., Hill-Yardin, E. L., & Hannan, A. J. (2015). A neuroligin-3 mutation implicated in autism causes abnormal aggression and increases repetitive behavior in mice. *Molecular Autism*, *6*(1), 1-11.

Busch, R.M., Srivastava, S., Hogue, O., Frazier, T.W., Klaas, P., Hardan, A., Martinez-Agosto, J.A., Sahin, M. and Eng, C. (2019). Neurobehavioral phenotype of autism spectrum disorder associated with germline heterozygous mutations in PTEN. *Translational Psychiatry*, *9*(1), 1-9.

Cruikshank, S. J., & Weinberger, N. M. (1996). Evidence for the Hebbian hypothesis in experience-dependent physiological plasticity of neocortex: a critical review. *Brain Research Reviews*, *22*(3), 191-228.

Chiossi, G., Costantine, M.M., Bytautiene, E., Kechichian, T., Hankins, G.D., Sbrana, E., Saade, G.R. & Longo, M. (2012). The effects of PGE1 and PGE2 on in vitro myometrial contractility and uterine structure. *American Journal of Perinatology*, *29*(8), 615.

Cajal, R. S. (1892) El nuevo concepto de la histología de los centros nerviosos. *La Revista de Ciencias Médicas de Barcelona*, *18*, 361–376.

Cajal, R. S. (1913). Sobre la degeneración y regeneración del sistema nervioso. *Imprenta de Hijos de Nicolás Moya, Madrid*, *2*.

Chauhan, Y. S., Lu, D. D., Sriramkumar, V., Khandelwal, S., Duarte, J. P., Payvadosi, N., Niknejad, A., & Hu, C. (2015). *FinFET modeling for IC simulation and design: using the BSIM-CMG standard*. Chapter 8 - Noise. Academic Press.

Chen, C., Magee, J. C., & Bazan, N. G. (2002). Cyclooxygenase-2 regulates prostaglandin E2 signaling in hippocampal long-term synaptic plasticity. *Journal of Neurophysiology*, *87*(6), 2851-2857.

Chen, Q., Panksepp, J. B., & Lahvis, G. P. (2009). Empathy is moderated by genetic background in mice. *PloS One*, *4*(2), e4387.

Christensen, D.L., Braun, K.V.N., Baio, J., Bilder, D., Charles, J., Constantino, J.N., Daniels, J., Durkin, M.S., Fitzgerald, R.T., Kurzius-Spencer, M. & Lee, L.C. (2018). Prevalence and characteristics of autism spectrum disorder among children aged 8 years—autism and developmental disabilities monitoring network, 11 sites, United States, 2012. *MMWR Surveillance Summaries*, *65*(13), 1.

Clifford, C. W., & Woodring, J. P. (1990). Methods for rearing the house cricket, Acheta domesticus (L.), along with baseline values for feeding rates, growth rates, development times, and blood composition. *Journal of Applied Entomology*, *109*(1-5), 1-14.

Coast, G. M., & Kay, I. A. I. N. (1994). The effects of Acheta diuretic peptide on isolated Malpighian tubules from the house cricket Acheta domesticus. *Journal of Experimental Biology*, *187*(1), 225-243.

Connor, S.A., Elegheert, J., Xie, Y. & Craig, A.M. (2019). Pumping the brakes: suppression of synapse development by MDGA–neuroligin interactions. *Current Opinion in Neurobiology*, *57*, 71-80.

Connor, S.A., Ammendrup-Johnsen, I., Chan, A.W., Kishimoto, Y., Murayama, C., Kurihara, N., Tada, A., Ge, Y., Lu, H., Yan, R. and LeDue, J.M. (2016). Altered cortical dynamics and cognitive function upon haploinsufficiency of the autism-linked excitatory synaptic suppressor MDGA2. *Neuron*, *91*(5), 1052-1068.

Cooper, R.A., Richter, F.R., Bays, P.M., Plaisted-Grant, K.C., Baron-Cohen, S. & Simons, J.S. (2017). Reduced hippocampal functional connectivity during episodic memory retrieval in autism. *Cerebral Cortex*, *27*(2), 888-902.

Courchesne, E., Mouton, P.R., Calhoun, M.E., Semendeferi, K., Ahrens-Barbeau, C., Hallet, M.J., Barnes, C.C. & Pierce, K. (2011). Neuron number and size in prefrontal cortex of children with autism. *Jama*, *306*(18), 2001-2010.

Crawford, D. (2021). *Neurobiology of Lipid Signalling in the Developing Brain: Link to Autism Spectrum Disorders*. Department of Biology Seminar. York University. March 22, 2021.

Cupolillo, D., Hoxha, E., Faralli, A., De Luca, A., Rossi, F., Tempia, F., & Carulli, D. (2016). Autistic-like traits and cerebellar dysfunction in Purkinje cell PTEN knock-out mice. *Neuropsychopharmacology*, *41*(6), 1457-1466.

Dachtler, J., Glasper, J., Cohen, R.N., Ivorra, J.L., Swiffen, D.J., Jackson, A.J., Harte, M.K., Rodgers, R.J. & Clapcote, S.J. (2014). Deletion of α-neurexin II results in autism-related behaviors in mice. *Translational Psychiatry*, *4*(11), pp.e484-e484.

DeVita, V. T., & Chu, E. (2008). A history of cancer chemotherapy. *Cancer Research*, *68*(21), 8643-8653.

Dhamne, S.C., Silverman, J.L., Super, C.E., Lammers, S.H., Hameed, M.Q., Modi, M.E., Copping, N.A., Pride, M.C., Smith, D.G., Rotenberg, A. & Crawley, J.N. (2017). Replicable in vivo physiological and behavioral phenotypes of the Shank3B null mutant mouse model of autism. *Molecular Autism*, *8*(1), 1-19.

Domanski, A. P., Booker, S. A., Wyllie, D. J., Isaac, J. T., & Kind, P. C. (2019). Cellular and synaptic phenotypes lead to disrupted information processing in Fmr1-KO mouse layer 4 barrel cortex. *Nature Communications*, *10*(1), 1-18.

Dutta, S., & Sengupta, P. (2016). Men and mice: relating their ages. *Life Sciences*, *152*, 244-248.

Elegheert, J., Cvetkovska, V., Clayton, A.J., Heroven, C., Vennekens, K.M., Smukowski, S.N., Regan, M.C., Jia, W., Smith, A.C., Furukawa, H. & Savas, J.N. (2017). Structural mechanism for modulation of synaptic neuroligin-neurexin signaling by MDGA proteins. *Neuron*, *95*(4), 896-913.

Etherton, M., Földy, C., Sharma, M., Tabuchi, K., Liu, X., Shamloo, M., Malenka, R.C. & Südhof, T.C. (2011). Autism-linked neuroligin-3 R451C mutation differentially alters hippocampal and cortical synaptic function. *Proceedings of the National Academy of Sciences*, *108*(33), 13764-13769.

Folstein, S. & Rutter, M. (1977). Infantile Autism: A Genetic Study of 21 Twin Pairs. *Journal of Child Psychology and Psychiatry, 18*, 297–321.

Foster, E. S., Signs, K. A., Marks, D. R., Kapoor, H., Casey, M., Stobierski, M. G., & Walker, E. D. (2006). Lymphocytic choriomeningitis in Michigan. *Emerging Infectious Diseases*, *12*(5), 851.

Fraser, M. M., Bayazitov, I. T., Zakharenko, S. S., & Baker, S. J. (2008). Pten deficiency in brain causes defects in synaptic structure, transmission and plasticity, and myelination abnormalities. *Neuroscience*, *151*(2), 476.

Frazier, T. W., Embacher, R., Tilot, A. K., Koenig, K., Mester, J., & Eng, C. (2015). Molecular and phenotypic abnormalities in individuals with germline heterozygous PTEN mutations and autism. *Molecular Psychiatry*, *20*(9), 1132-1138.

Gaffney, G. R., Kuperman, S., Tsai, L. Y. & Minchin, S. (1989). Forebrain Structure in Infantile Autism. *Journal of the American Academy of Child & Adolescent Psychiatry, 28*, 534–537.

Gage, F. H. (2004). Structural plasticity of the adult brain. *Dialogues in Clinical Neuroscience, 6*, 135.

Gol, A., & Faibish, G. M. (1967). Effects of human hippocampal ablation. *Journal of Neurosurgery*, *26*(4), 390-398.

Gong, X., & Wang, H. (2015). SHANK1 and autism spectrum disorders. *Science China Life sciences*, *58*(10), 985-990.

Gonzalez, C. H., Marques-Dias, M. J., Kim, C. A., Sugayama, S. M., Da Paz, J. A., Huson, S. M., & Holmes, L. B. (1998). Congenital abnormalities in Brazilian children associated with misoprostol misuse in first trimester of pregnancy. *The Lancet*, *351*(9116), 1624-1627.

Grayton, H. M., Missler, M., Collier, D. A. & Fernandes, C. (2013). Altered Social Behaviours in Neurexin 1α Knockout Mice Resemble Core Symptoms in Neurodevelopmental Disorders. *PLoS One*, 8, e67114.

Greydanus, D. E., & Toledo-Pereyra, L. H. (2012). Historical perspectives on autism: Its past record of discovery and its present state of solipsism, skepticism, and sorrowful suspicion. *Pediatric Clinics*, *59*(1), 1-11.

Hafting, T., Fyhn, M., Molden, S., Moser, M. B., & Moser, E. I. (2005). Microstructure of a spatial map in the entorhinal cortex. *Nature*, *436*(7052), 801-806.

Hallmayer, J., Cleveland, S., Torres, A., Phillips, J., Cohen, B., Torigoe, T., Miller, J., Fedele, A., Collins, J., Smith, K. & Lotspeich, L. (2011). Genetic heritability and shared environmental factors among twin pairs with autism. *Archives of General Psychiatry*, *68*(11), 1095-1102.

Hazlett, H. C., Poe, M., Gerig, G., Smith, R. G., Provenzale, J., Ross, A., Gilmore, J. and Piven, J. (2005). Magnetic resonance imaging and head circumference study of brain size in autism: birth through age 2 years. *Archives of General Psychiatry*, *62*(12), 1366-1376.

Hebb, D. O. (1949). The first stage of perception: growth of the assembly. *The Organization of Behavior*, *4*, 60-78.

Huang, E. P. (1998). Synaptic plasticity: going through phases with LTP. *Current Biology*, 8, R350-R352.

Huber, K. M., Gallagher, S. M., Warren, S. T., & Bear, M. F. (2002). Altered synaptic plasticity in a mouse model of fragile X mental retardation. *Proceedings of the National Academy of Sciences*, *99*(11), 7746-7750.

Hung, A.Y., Futai, K., Sala, C., Valtschanoff, J.G., Ryu, J., Woodworth, M.A., Kidd, F.L., Sung, C.C., Miyakawa, T., Bear, M.F. & Weinberg, R.J. (2008). Smaller dendritic spines, weaker synaptic transmission, but enhanced spatial learning in mice lacking Shank1. *Journal of Neuroscience*, *28*(7), 1697-1708.

Hutsler, J. J., Love, T. & Zhang, H. (2007). Histological and Magnetic Resonance Imaging Assessment of Cortical Layering and Thickness in Autism Spectrum Disorders. *Biological Psychiatry 61*, 449–457.

Jacobs, G. A., Miller, J. P., & Aldworth, Z. (2008). Computational mechanisms of mechanosensory processing in the cricket. *Journal of Experimental Biology*, *211*(11), 1819-1828.

Johns, P. (2014). Neurons and glial cells. *Clinical Neuroscience: An Illustrated Colour Text*, *5*, 61.

Kalueff, A. V., Minasyan, A., Keisala, T., Shah, Z. H., & Tuohimaa, P. (2006). Hair barbering in mice: implications for neurobehavioural research. *Behavioural Processes*, *71*(1), 8-15.

Kandel, E. R. (2001). The molecular biology of memory storage: a dialogue between genes and synapses. *Science* 294, 1030-1038.

Kanner, L. (1943). Autistic disturbances of affective contact. *Nervous Child*, *2*, 217-250.

Kerr, D. (2009). Kerr Scientific Instruments Tissue Recording System Owner's Guide. *New Zealand: Kerr Scientific Instruments*.

Koenig, C. M., Walker, C. K., Qi, L., Pessah, I. N., & Berman, R. F. (2012). Lack of evidence for neonatal misoprostol neurodevelopmental toxicity in C57BL6/J mice. *PloS One*, *7*(6), e38911.

Kuhn, M., Wolf, E., Maier, J. G., Mainberger, F., Feige, B., Schmid, H., Bürklin, J., Maywald, S., Mall, V., Jung, N.H., & Reis, J. (2016). Sleep recalibrates homeostatic and associative synaptic plasticity in the human cortex. *Nature Communications*, *7*, 12455.

Kumar, D. (1990). Moebius syndrome. *Journal of Medical Genetics*, *27*(2), 122.

Lee, F. H., Lai, T. K., Su, P., & Liu, F. (2019). Altered cortical Cytoarchitecture in the Fmr1 knockout mouse. *Molecular Brain*, *12*(1), 1-12.

Lee, J., Chung, C., Ha, S., Lee, D., Kim, D. Y., Kim, H., & Kim, E. (2015). Shank3-mutant mice lacking exon 9 show altered excitation/inhibition balance, enhanced rearing, and spatial memory deficit. *Frontiers in Cellular Neuroscience*, *9*, 94.

Lee, K. Y., Jewett, K. A., Chung, H. J., & Tsai, N. P. (2018). Loss of fragile X protein FMRP impairs homeostatic synaptic downscaling through tumor suppressor p53 and ubiquitin E3 ligase Nedd4-2. *Human Molecular Genetics*, *27*(16), 2805-2816.

Legler, D. F., Bruckner, M., Uetz-von Allmen, E., & Krause, P. (2010). Prostaglandin E2 at new glance: novel insights in functional diversity offer therapeutic chances. *The International Journal of Biochemistry & Cell Biology*, *42*(2), 198-201.

Lein, P. J., Barnhart, C. D., & Pessah, I. N. (2011). Acute hippocampal slice preparation and hippocampal slice cultures. *In Vitro Neurotoxicology* (pp. 115-134). Humana Press, Totowa, NJ.

Letellier, M., Szíber, Z., Chamma, I., Saphy, C., Papasideri, I., Tessier, B., Sainlos, M., Czöndör, K. and Thoumine, O. (2018). A unique intracellular tyrosine in neuroligin-1 regulates AMPA receptor recruitment during synapse differentiation and potentiation. *Nature Communications*, *9*(1), 1-17.

Lewine, J.D., Andrews, R., Chez, M., Patil, A.A., Devinsky, O., Smith, M., Kanner, A., Davis, J.T., Funke, M., Jones, G. and Chong, B. (1999). Magnetoencephalographic patterns of epileptiform activity in children with regressive autism spectrum disorders. *Pediatrics*, *104*(3), 405-418.

Lugo, J. N., Smith, G. D., Morrison, J. B., & White, J. (2013). Deletion of PTEN produces deficits in conditioned fear and increases fragile X mental retardation protein. *Learning & Memory*, *20*(12), 670-673.

Lugo, J. N., Smith, G. D., Arbuckle, E. P., White, J., Holley, A. J., Floruta, C. M., Ahmed, N., Gomez, M. C. & Okonkwo, O. (2014). Deletion of PTEN produces autism-like behavioral deficits and alterations in synaptic proteins. *Frontiers in Molecular Neuroscience*, *7*, 27.

Lynch, M. A. (2004). Long-Term Potentiation and Memory. *Physiological Reviews. 84*, 87–136.

MacPherson, P., McGaffigan, R., Wahlsten, D., & Nguyen, P. V. (2008). Impaired fear memory, altered object memory and modified hippocampal synaptic plasticity in split-brain mice. *Brain Research*, *1210*, 179-188.

Mao, W., Watanabe, T., Cho, S., Frost, J. L., Truong, T., Zhao, X., & Futai, K. (2015). Shank1 regulates excitatory synaptic transmission in mouse hippocampal parvalbumin-expressing inhibitory interneurons. *European Journal of Neuroscience*, *41*(8), 1025-1035.

Marques-Dias, M. J., Gonzalez, C. H., & Rosemberg, S. (2003). Möbius sequence in children exposed in utero to misoprostol: neuropathological study of three cases. *Birth Defects Research Part A: Clinical and Molecular Teratology*, *67*(12), 1002-1007.

Marsden, M. D. (2020). Benefits and limitations of humanized mice in HIV persistence studies. *Retrovirology*, *17*, 1-6.

Martínez-Cerdeño, V. (2017). Dendrite and spine modifications in autism and related neurodevelopmental disorders in patients and animal models. *Developmental Neurobiology*, *77*(4), 393-404.

Mendenhall, B., & Murphey, R. K. (1974). The morphology of cricket giant interneurons. *Journal of Neurobiology*, *5*(6), 565-580.

Meyza, K. Z., & Blanchard, D. C. (2017). The BTBR mouse model of idiopathic autism – Current view on mechanisms. *Neuroscience & Biobehavioral Reviews*, *76*, 99-110.

Milner, B., Corkin, S., & Teuber, H. L. (1968). Further analysis of the hippocampal amnesic syndrome: 14-year follow-up study of HM. *Neuropsychologia*, *6*(3), 215-234.

Molecular Devices. (2012). The Axon Guide, A Guide to Electrophysiology & Biophysics Laboratory Techniques. *Sunnyvale: MDS Analytical Technologies*.

Morrissey, R. E., & Edwards, J. S. (1981). Effects of ethanol on sensory processing in the central nervous system of an insect: the cercal-to-giant interneuron system of the house cricket. *Comparative Biochemistry and Physiology Part C: Comparative Pharmacology*, *70*(2), 159-169.

Nelson, S. B., & Valakh, V. (2015). Excitatory/inhibitory balance and circuit homeostasis in autism spectrum disorders. *Neuron*, *87*(4), 684-698.

Ofner, M., Coles, A., Decou, M.L., Do, M.T., Bienek, A., Snider, J. & Ugnat, A. (2018). *Autism spectrum disorder among children and youth in Canada 2018*. Ottawa, ON: Public Health Agency of Canada.

Ogawa, H., & Mitani, R. (2015). Spatial dynamics of action potentials estimated by dendritic Ca^{2+} signals in insect projection neurons. *Biochemical and Biophysical Research Communications*, *467*(2), 185-190.

O'Keefe, J., & Dostrovsky, J. (1971). The hippocampus as a spatial map: preliminary evidence from unit activity in the freely-moving rat. *Brain Research*.

Ousley, O. & Tracy C. (2014). Autism spectrum disorder: defining dimensions and subgroups. *Current Developmental Disorders Reports 1*, 20-28.

Pastuszak, A. L., Schüler, L., Speck-Martins, C. E., Coelho, K. E. F., Cordello, S. M., Vargas, F., Brunoni, D., Schwarz, I. V., Larrandaburu, M., Safattle, H. & Meloni, V. F. (1998). Use of misoprostol during pregnancy and Möbius' syndrome in infants. *New England Journal of Medicine*, *338*(26), 1881-1885.

Peça, J., Feliciano, C., Ting, J. T., Wang, W., Wells, M. F., Venkatraman, T. N., Lascola, C. D., Fu, Z. & Feng, G. (2011). Shank3 mutant mice display autistic-like behaviours and striatal dysfunction. *Nature*, *472*(7344), 437-442.

Philippe, A., Martinez, M., Guilloud-Bataille, M., Gillberg, C., Råstam, M., Sponheim, E., Coleman, M., Zappella, M., Aschauer, H., Van Maldergem, L. & Penet, C. (1999). Genome-wide scan for autism susceptibility genes. *Human Molecular Genetics*, *8*(5), 805-812.

Radyushkin, K., Hammerschmidt, K., Boretius, S., Varoqueaux, F., El-Kordi, A., Ronnenberg, A., Winter, D., Frahm, J., Fischer, J., Brose, N. & Ehrenreich, H. (2009). Neuroligin-3-deficient mice: model of a monogenic heritable form of autism with an olfactory deficit. *Genes, Brain and Behavior*, *8*(4), 416-425.

Rai-Bhogal, R., Wong, C., Kissoondoyal, A., Davidson, J., Li, H., & Crawford, D. A. (2018). Maternal exposure to prostaglandin E2 modifies expression of Wnt genes in mouse brain – An autism connection. *Biochemistry and Biophysics Reports*, *14*, 43-53.

Rajmohan, V., & Mohandas, E. (2007). The limbic system. *Indian Journal of Psychiatry*, *49*(2), 132.

Ramakers, G. J. A., Corner, M. A., & Habets, A. M. M. C. (1990). Development in the absence of spontaneous bioelectric activity results in increased stereotyped burst firing in cultures of dissociated cerebral cortex. *Experimental Brain Research*, *79*(1), 157-166.

Rausche, G., Igelmund, P., & Heinemann, U. (1990). Effects of changes in extracellular potassium, magnesium and calcium concentration on synaptic transmission in area CA1 and the dentate gyrus of rat hippocampal slices. *Pflügers Archiv*, *415*(5), 588-593.

Rothwell, P.E., Fuccillo, M.V., Maxeiner, S., Hayton, S.J., Gokce, O., Lim, B.K., Fowler, S.C., Malenka, R.C. & Südhof, T.C. (2014). Autism-associated neuroligin-3 mutations commonly impair striatal circuits to boost repetitive behaviors. *Cell*, *158*(1), 198-212.

Sattelle, D. B., Lummis, S. C., Wong, J. F., & Rauh, J. J. (1991). Pharmacology of insect GABA receptors. *Neurochemical Research*, *16*(3), 363-374.

Scoville, W. B., & Milner, B. (1957). Loss of recent memory after bilateral hippocampal lesions. *Journal of Neurology, Neurosurgery, and Psychiatry*, *20*(1), 11.

Semple, B. D., Blomgren, K., Gimlin, K., Ferriero, D. M., & Noble-Haeusslein, L. J. (2013). Brain development in rodents and humans: Identifying benchmarks of maturation and vulnerability to injury across species. *Progress in Neurobiology*, *106*, 1-16.

Shah, B., Pattanayak, R. D., & Sagar, R. (2014). The study of patient Henry Molaison and what it taught us over past 50 years: Contributions to neuroscience. *Journal of Mental Health and Human Behaviour*, *19*(2), 91.

Shin, W., Kweon, H., Kang, R., Kim, D., Kim, K., Kang, M., Kim, S. Y., Hwang, S. N., Kim, J. Y., Yang, E. & Kim, H. (2019). Scn2a haploinsufficiency in mice suppresses hippocampal neuronal excitability, excitatory synaptic drive, and long-term potentiation, and spatial learning and memory. *Frontiers in Molecular Neuroscience*, *12*, 145.

Silverman, J. L., Turner, S. M., Barkan, C. L., Tolu, S. S., Saxena, R., Hung, A. Y., Sheng, M. & Crawley, J. N. (2011). Sociability and motor functions in Shank1 mutant mice. *Brain Research*, *1380*, 120-137.

Soderlund, D. M., Clark, J. M., Sheets, L. P., Mullin, L. S., Piccirillo, V. J., Sargent, D., Stevens, J.T., & Weiner, M. L. (2002). Mechanisms of pyrethroid neurotoxicity: implications for cumulative risk assessment. *Toxicology*, *171*(1), 3-59.

Sperow, M., Berry, R. B., Bayazitov, I. T., Zhu, G., Baker, S. J., & Zakharenko, S. S. (2012). Phosphatase and tensin homologue (PTEN) regulates synaptic plasticity independently of its effect on neuronal morphology and migration. The *Journal of Physiology*, *590*(4), 777-792.

Squire, L. R. (2009). The legacy of patient HM for neuroscience. *Neuron*, *61*(1), 6-9.

Stecker, M. (2017). Factors Affecting Stimulus Artifact: Solution Factors. *EC Neurology*, *5*, 52-61.

Steensma, D. P., Kyle, R. A., & Shampo, M. A. (2010). Abbie Lathrop, the "mouse woman of Granby": rodent fancier and accidental genetics pioneer. *Mayo Clinic Proceedings*, *85*(11), e83.

Stenseth, N.C., Leirs, H., Skonhoft, A., Davis, S.A., Pech, R.P., Andreassen, H.P., Singleton, G.R., Lima, M., Machang'u, R.S., Makundi, R.H. & Zhang, Z. (2003). Mice, rats, and people: the bio-economics of agricultural rodent pests. *Frontiers in Ecology and the Environment*, *1*(7), 367-375.

Strömland, K., Sjögreen, L., Miller, M., Gillberg, C., Wentz, E., Johansson, M., Nylén, O., Danielsson, A., Jacobsson, C., Andersson, J. & Fernell, E. (2002). Möbius sequence — a Swedish multidiscipline study. *European Journal of Paediatric Neurology*, *6*(1), 35-45.

Sultana, R., Ogundele, O. M., & Lee, C. C. (2019). Contrasting characteristic behaviours among common laboratory mouse strains. *Royal Society Open Science*, *6*(6), 190574.

Sungur, A. Ö., Vörckel, K. J., Schwarting, R. K., & Wöhr, M. (2014). Repetitive behaviors in the Shank1 knockout mouse model for autism spectrum disorder: developmental aspects and effects of social context. *Journal of Neuroscience Methods*, *234*, 92-100.

Sweatt, J. D. (2009). Long-Term Potentiation — A Candidate Cellular Mechanism for Information Storage in the Central Nervous System. *Mechanisms of Memory*, *7*, 151-189.

Tabuchi, K., Blundell, J., Etherton, M. R., Hammer, R. E., Liu, X., Powell, C. M., & Südhof, T. C. (2007). A neuroligin-3 mutation implicated in autism increases inhibitory synaptic transmission in mice. *Science, 318*(5847), 71-76.

Takarae, Y. & Sweeney, J. (2017). Neural Hyperexcitability in Autism Spectrum Disorders. *Brain Sciences. 7*, 129.

Takeuchi, K., Gertner, M. J., Zhou, J., Parada, L. F., Bennett, M. V. & Zukin, R. S. (2013). Dysregulation of synaptic plasticity precedes appearance of morphological defects in a Pten conditional knockout mouse model of autism. *Proceedings of the National Academy of Sciences*, *110*(12), 4738-4743.

Tamiji, J., & Crawford, D. A. (2010). Prostaglandin E2 and misoprostol induce neurite retraction in Neuro-2a cells. *Biochemical and Biophysical Research Communications*, *398*(3), 450-456.

Tang, G., Gudsnuk, K., Kuo, S. H., Cotrina, M. L., Rosoklija, G., Sosunov, A., Sonders, M. S., Kanter, E., Castagna, C., Yamamoto, A. & Yue, Z. (2014). Loss of mTOR-dependent macroautophagy causes autistic-like synaptic pruning deficits. *Neuron*, *83*(5), 1131-1143.

Taoufik, E., Kouroupi, G., Zygogianni, O. & Matsas, R. (2018). Synaptic dysfunction in neurodegenerative and neurodevelopmental diseases: an overview of induced pluripotent stem-cell-based disease models. *Open Biology*, *8*(9), 180138.

Tatavarty, V., Pacheco, A. T., Kuhnle, C. G., Lin, H., Koundinya, P., Miska, N. J., Hengen, K. B., Wagner, F. F., Van Hooser, S. D. & Turrigiano, G. G. (2020). Autism-associated Shank3 is essential for homeostatic compensation in rodent V1. *Neuron*, *106*(5), 769-777.

Tsumoto, T. (1993). Long-term depression in cerebral cortex: a possible substrate of "forgetting" that should not be forgotten. *Neuroscience Research*, *16*(4), 263-270.

Tuchman, R., & Rapin, I. (2002). Epilepsy in autism. *The Lancet Neurology*, *1*(6), 352-358.

Turrigiano, G. G., Leslie, K. R., Desai, N. S., Rutherford, L. C., & Nelson, S. B. (1998). Activity-dependent scaling of quantal amplitude in neocortical neurons. *Nature*, *391*(6670), 892-896.

Turrigiano, G. G., & Nelson, S. B. (2004). Homeostatic plasticity in the developing nervous system. *Nature Reviews Neuroscience*, *5*(2), 97-107.

Van Den Pol, A. N., Obrietan, K., & Belousov, A. (1996). Glutamate hyperexcitability and seizure-like activity throughout the brain and spinal cord upon relief from chronic glutamate receptor blockade in culture. *Neuroscience*, *74*(3), 653-674.

Ventola, P., Lei, J., Paisley, C., Lebowitz, E., & Silverman, W. (2017). Parenting a child with ASD: Comparison of parenting style between ASD, anxiety, and typical development. *Journal of Autism and Developmental Disorders, 47*(9), 2873-2884.

Villers, A., & Ris, L. (2013). Improved preparation and preservation of hippocampal mouse slices for a very stable and reproducible recording of long-term potentiation. *Journal of Visualized Experiments: JoVE,* (76).

Walther, H., Lambert, J. D. C., Jones, R. S. G., Heinemann, U., & Hamon, B. (1986). Epileptiform activity in combined slices of the hippocampus, subiculum and entorhinal cortex during perfusion with low magnesium medium. *Neuroscience Letters, 69*(2), 156-161.

Wang, X., McCoy, P. A., Rodriguiz, R. M., Pan, Y., Je, H. S., Roberts, A. C., Kim, C. J., Berrios, J., Colvin, J. S., Bousquet-Moore, D. & Lorenzo, I. (2011). Synaptic dysfunction and abnormal behaviors in mice lacking major isoforms of Shank3. *Human Molecular Genetics, 20*(15), 3093-3108.

Weissbrod, L., Marshall, F. B., Valla, F. R., Khalaily, H., Bar-Oz, G., Auffray, J. C., Vigne, J. D. & Cucchi, T. (2017). Origins of house mice in ecological niches created by settled hunter-gatherers in the Levant 15,000 y ago. *Proceedings of the National Academy of Sciences*, *114*(16), 4099-4104.

Weston, M. C., Chen, H., & Swann, J. W. (2014). Loss of mTOR repressors Tsc1 or Pten has divergent effects on excitatory and inhibitory synaptic transmission in single hippocampal neuron cultures. *Frontiers in Molecular Neuroscience, 7*, 1.

Wing, L. (1997). The history of ideas on autism: legends, myths and reality. *Autism, 1*(1), 13-23.

Wolff, S. (2004). The history of autism. *European Child & Adolescent Psychiatry*, *13*(4), 201-208.

Zhong, S., Ding, W., Sun, L., Lu, Y., Dong, H., Fan, X., Liu, Z., Chen, R., Zhang, S., Ma, Q. & Tang, F. (2020). Decoding the development of the human hippocampus. *Nature, 577*(7791), 531-536.